Supporting Information for:

"Probing Borafluorene B-C Bond Insertion With Gold Acetylide and Azide"

Yijie Li[†], *Yu-Hsuan Shen*[‡], *Alec M. Esper*[‡], *John R. Tidwell*[†], *Adam S. Veige*[‡*], *Caleb D. Martin*[†*]

† Baylor University, Department of Chemistry and Biochemistry, One Bear Place #97348, Waco, TX 76798

‡ University of Florida, Department of Chemistry, Center for Catalysis, Gainesville, FL 32611, United States

Author to address correspondence: Caleb D. Martin (caleb_d_martin@baylor.edu)

Table of Contents

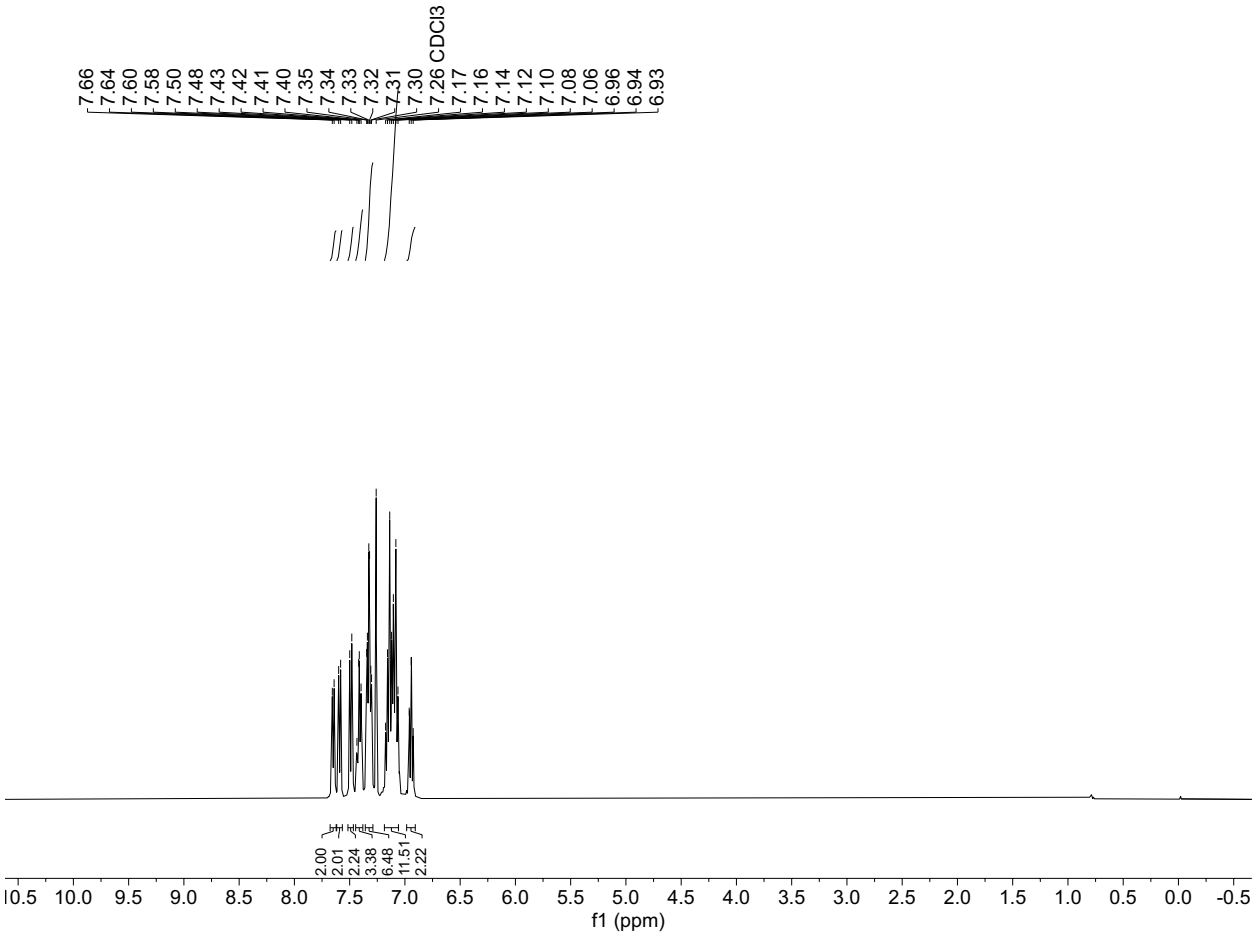

Figure S1. ^{1}H NMR spectrum of **2** in $CDCl_3$.

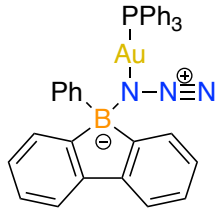

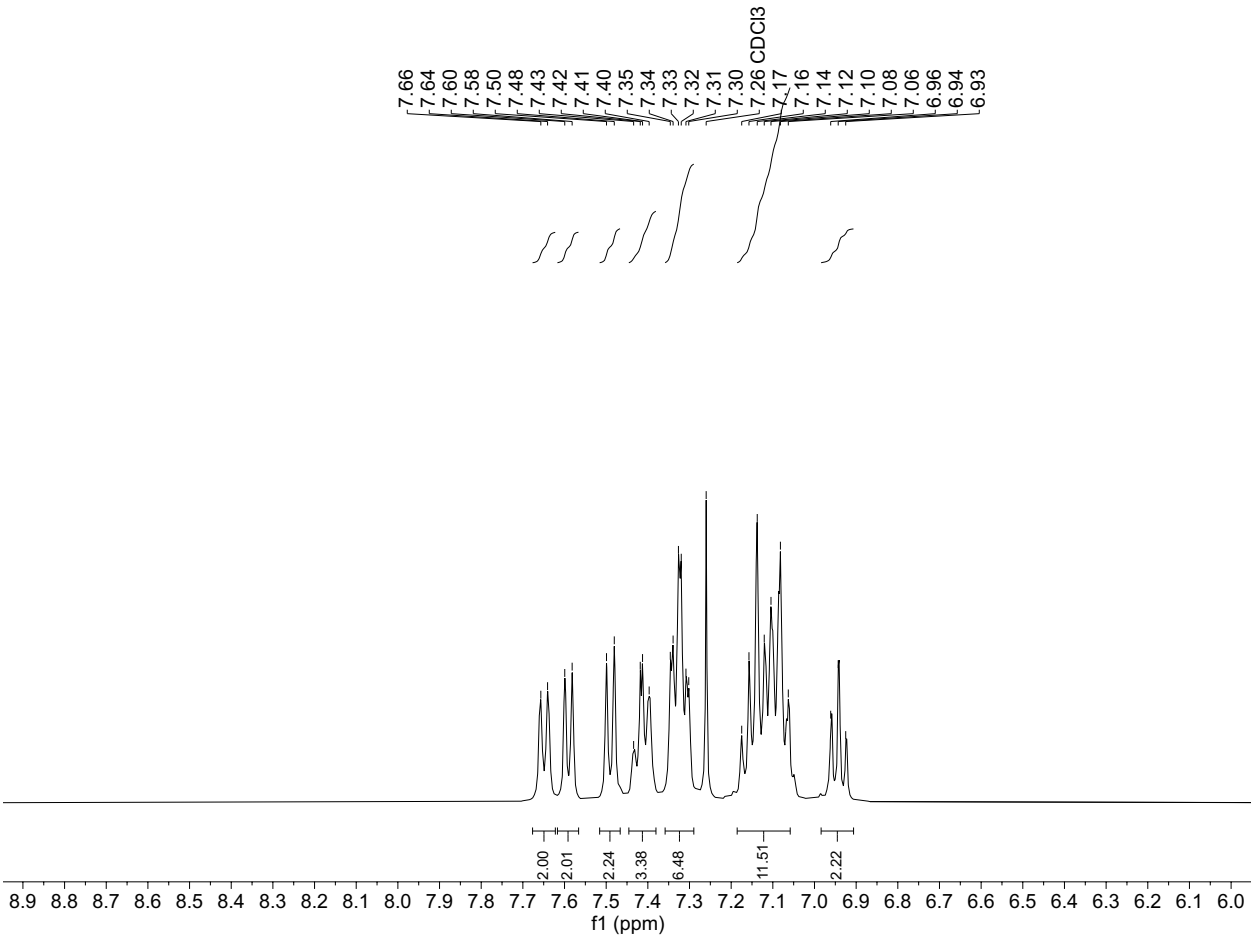

Figure S2. Expanded aryl region of ^{1}H NMR spectrum of **2** in $CDCl_3$.

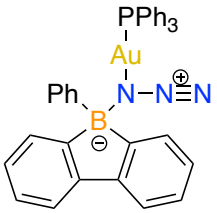

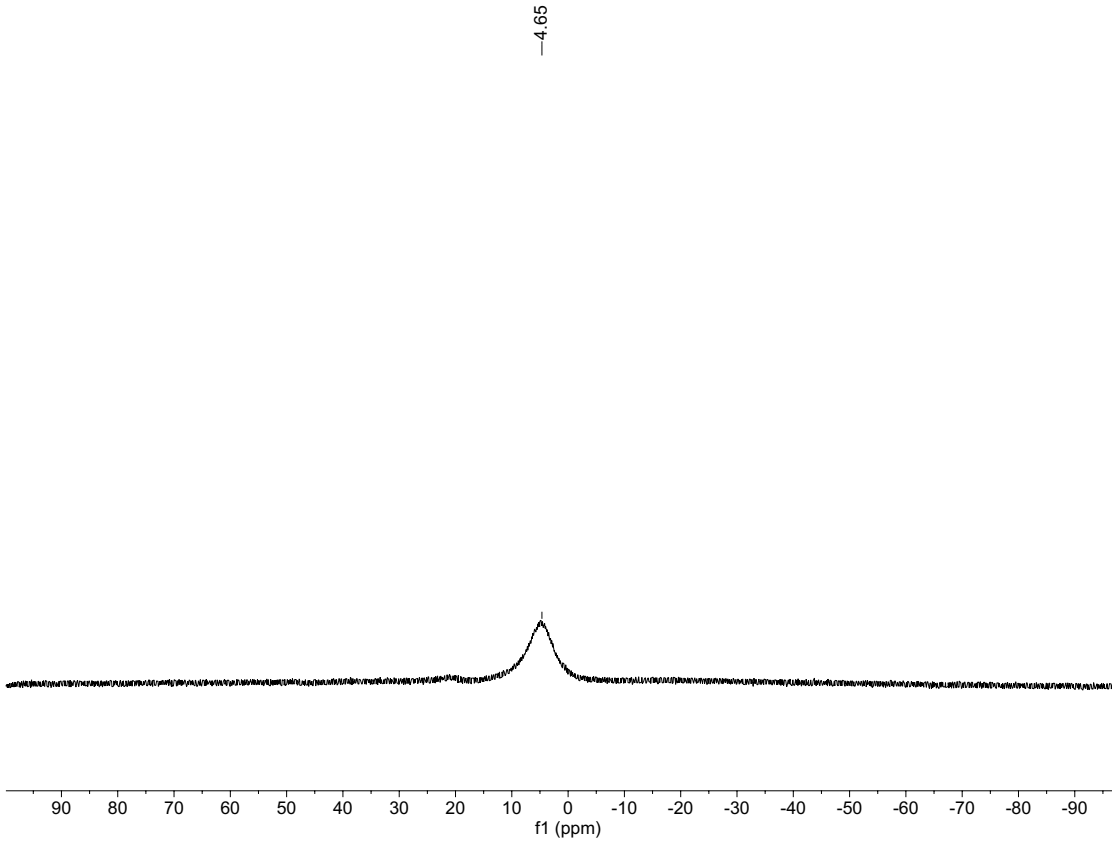

Figure S3. $^{11}B\{^{1}H\}$ NMR spectrum of **2** in $CDCl_3$.

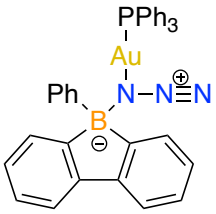

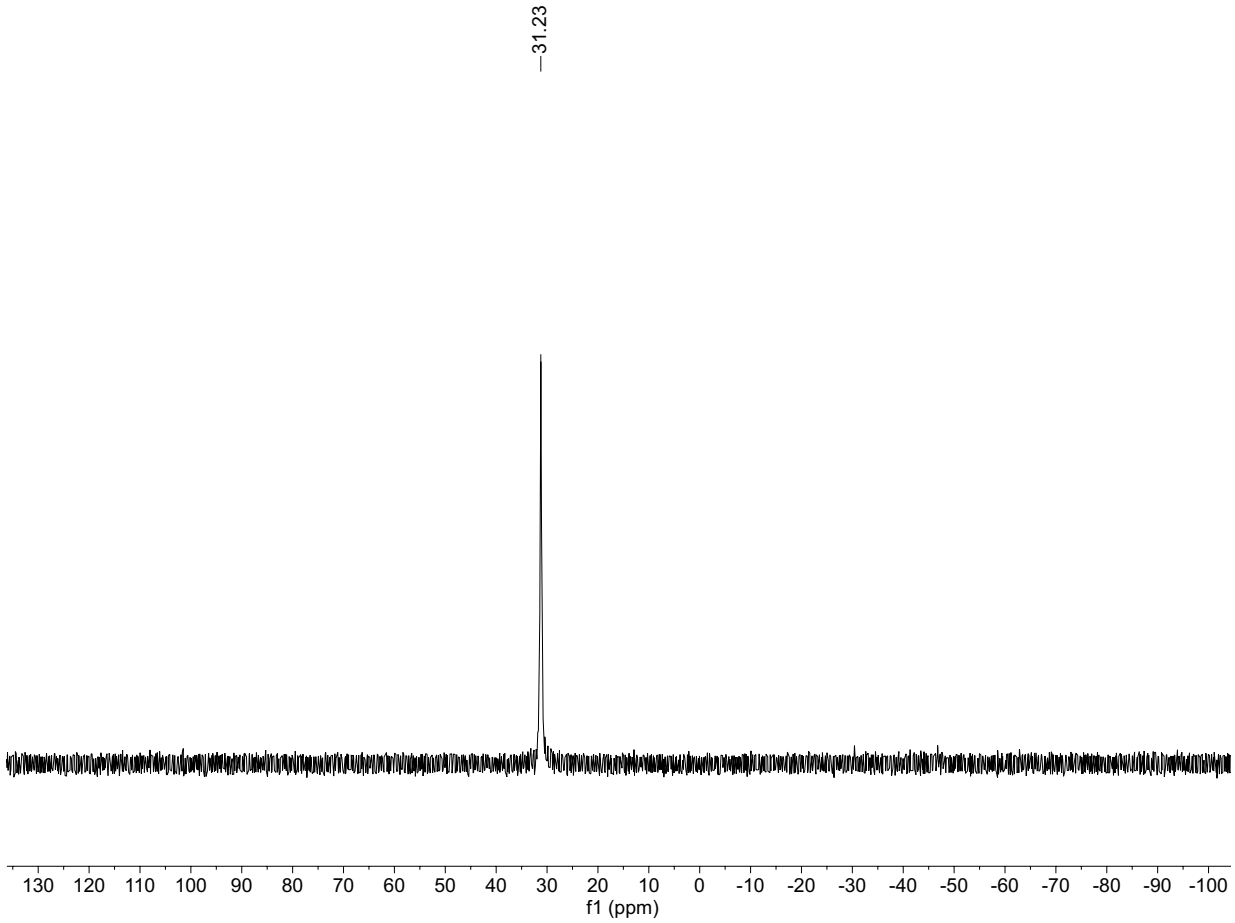

Figure S4. $^{31}P\{^{1}H\}$ NMR spectrum of **2** in $CDCl_3$.

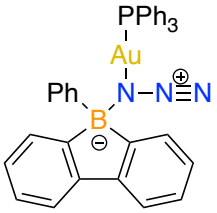

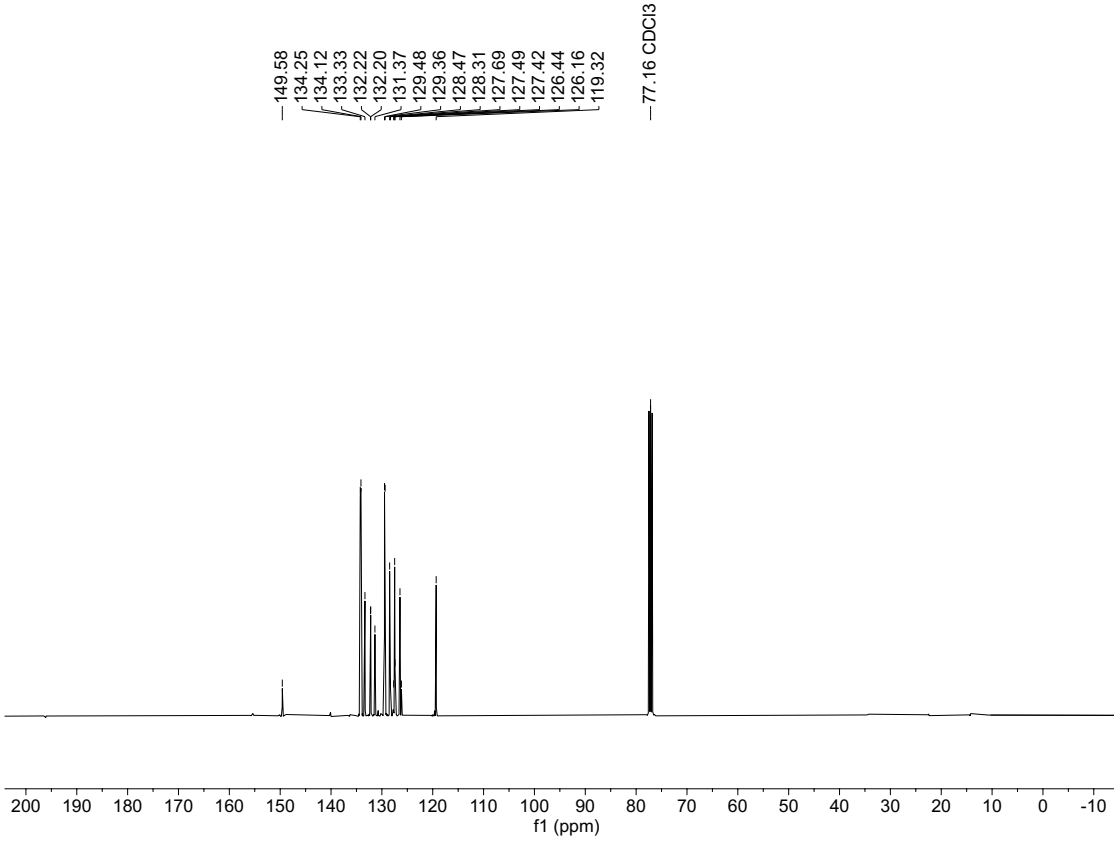

Figure S5. $^{13}C\{^{1}H\}$ NMR spectrum of **2** in $CDCl_3$.

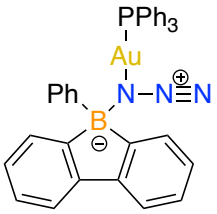

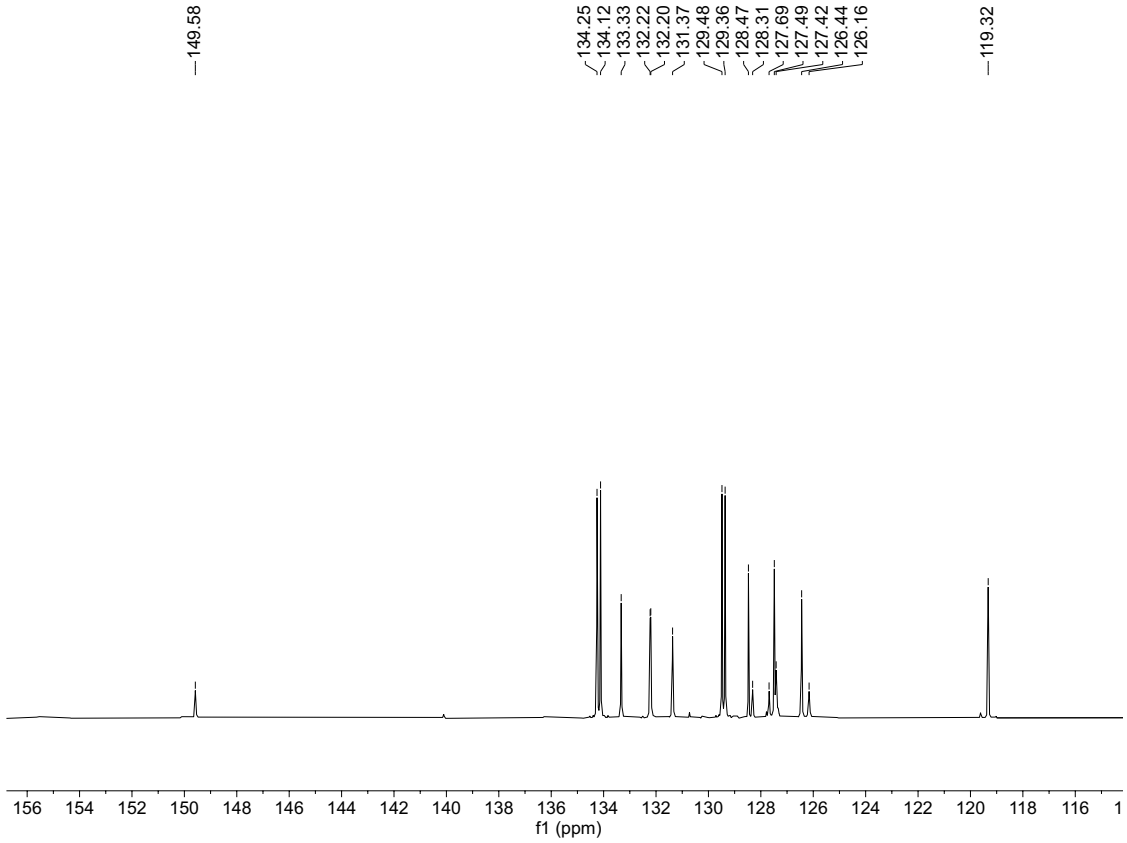

Figure S6. Expanded aryl region of $^{13}C\{^{1}H\}$ NMR spectrum of **2** in $CDCl_3$.

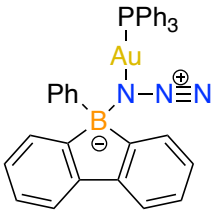

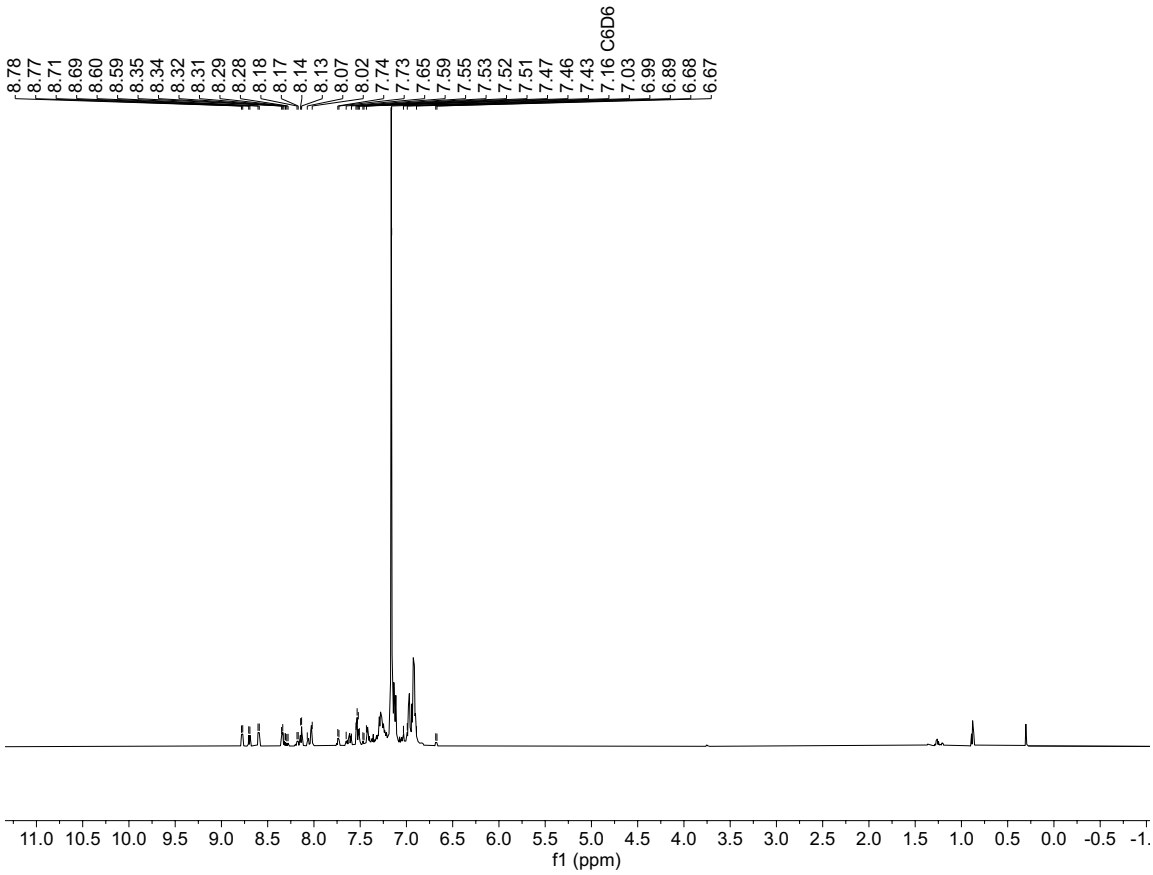

Figure S7. ^{1}H NMR spectrum of **2** after exposure under UV = 254 nm for 24 h in C_6D_6.

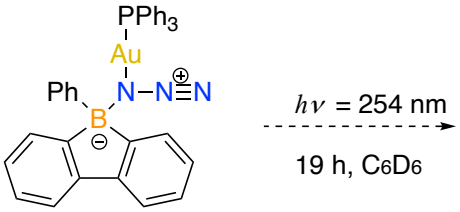

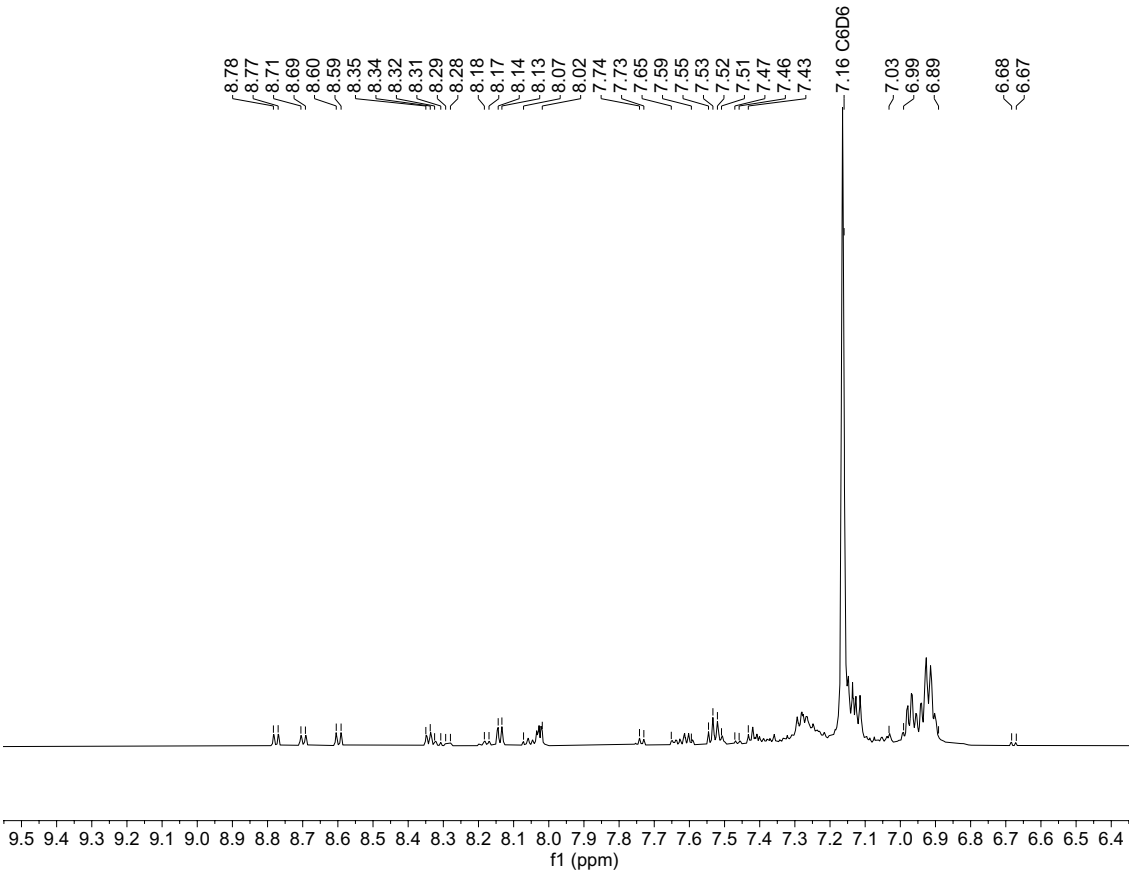

Figure S8. Expanded aryl region of ^{1}H NMR spectrum of **2** after exposure under UV = 254 nm for 24 h in C_6D_6.

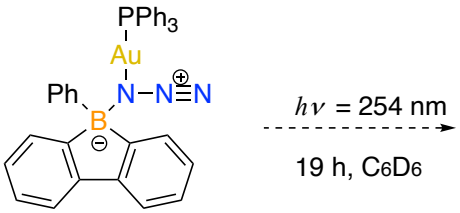

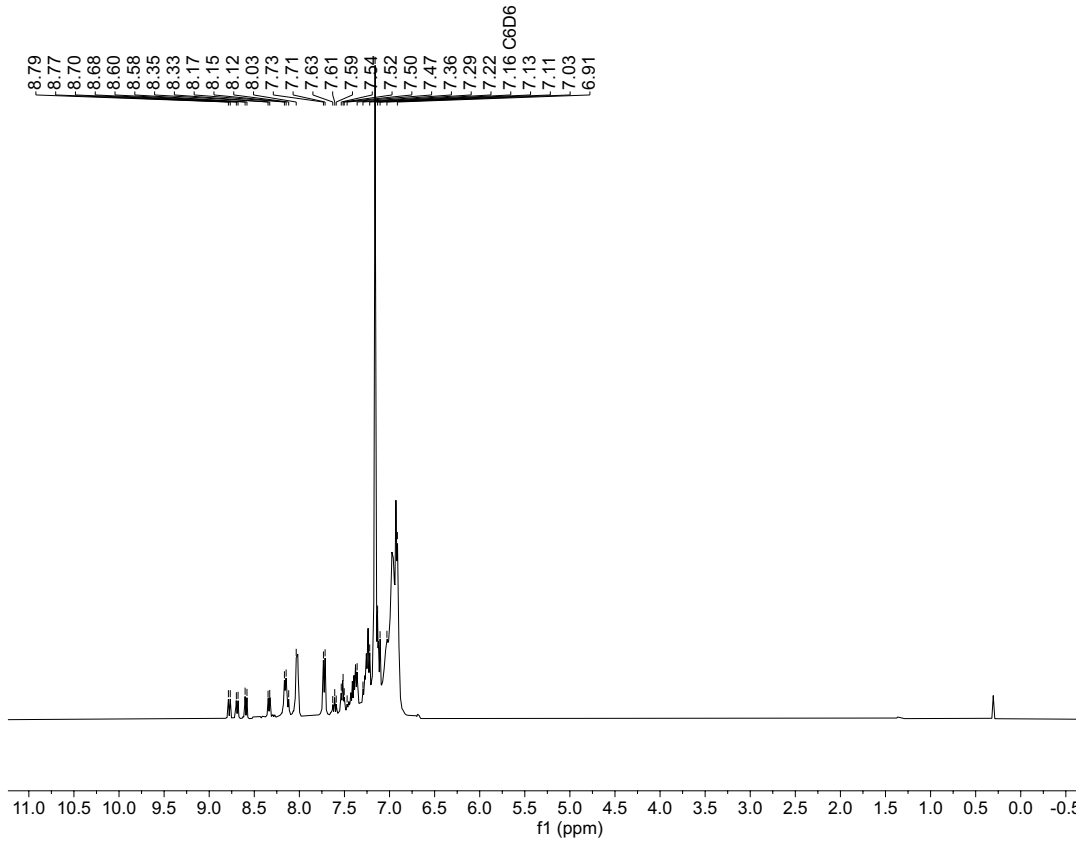

Figure S9. ^{1}H NMR spectrum of **2** after heating at 50 °C for 19 h in C_6D_6.

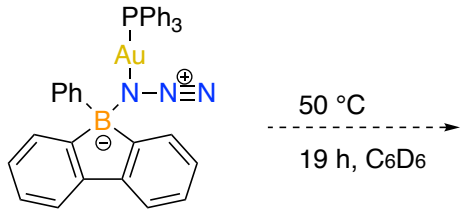

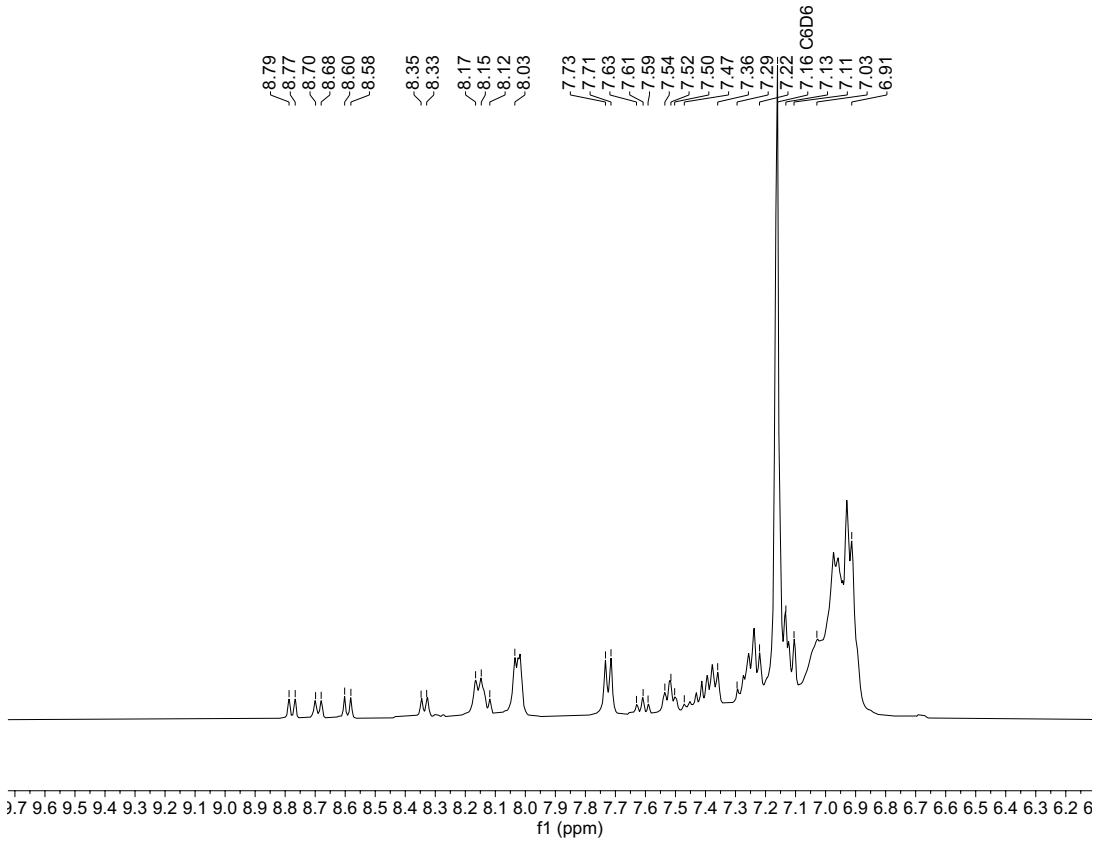

Figure S10. Expanded aryl region of ^{1}H NMR spectrum of **2** after heating at 50 °C for 19 h in C_6D_6.

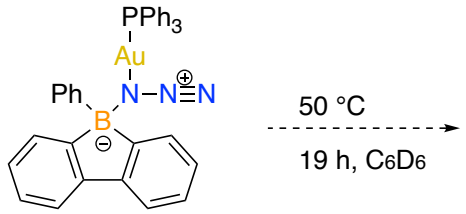

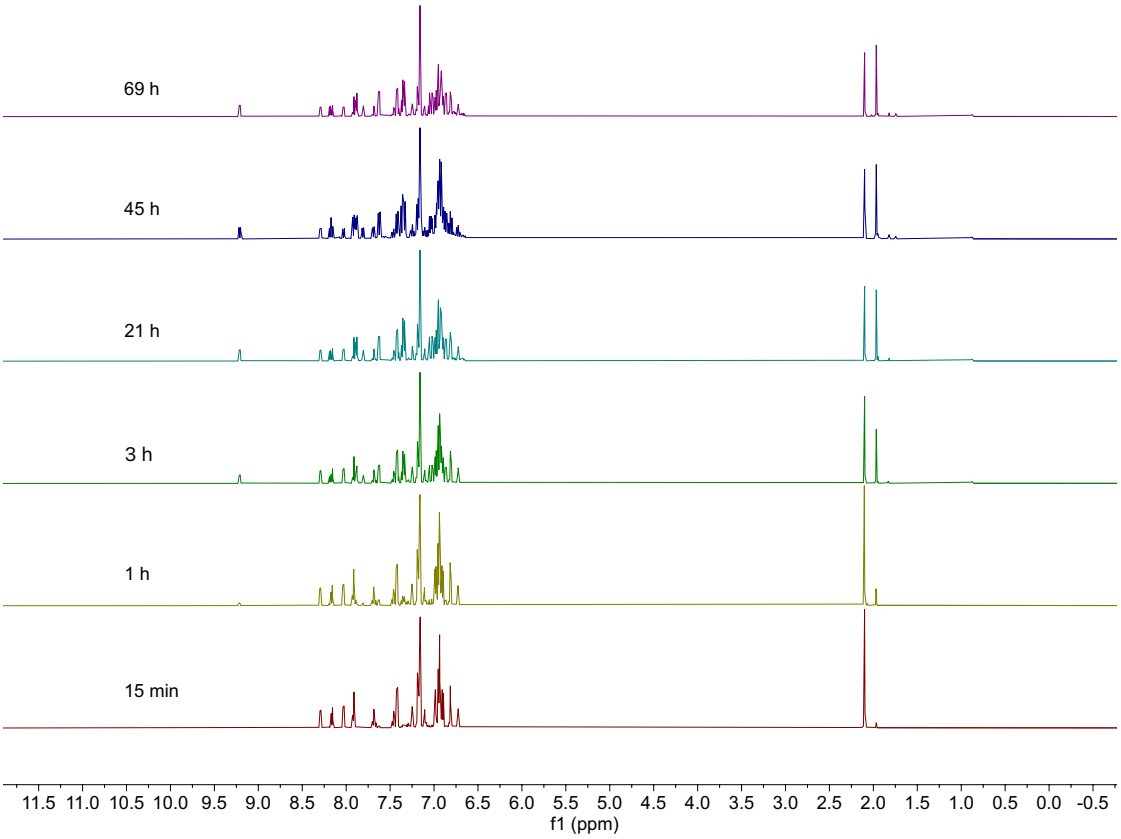

Figure S11. ^{1}H NMR spectra of reaction between **1** and Ph_3PAu-C≡C-*p*-tol in C_6D_6

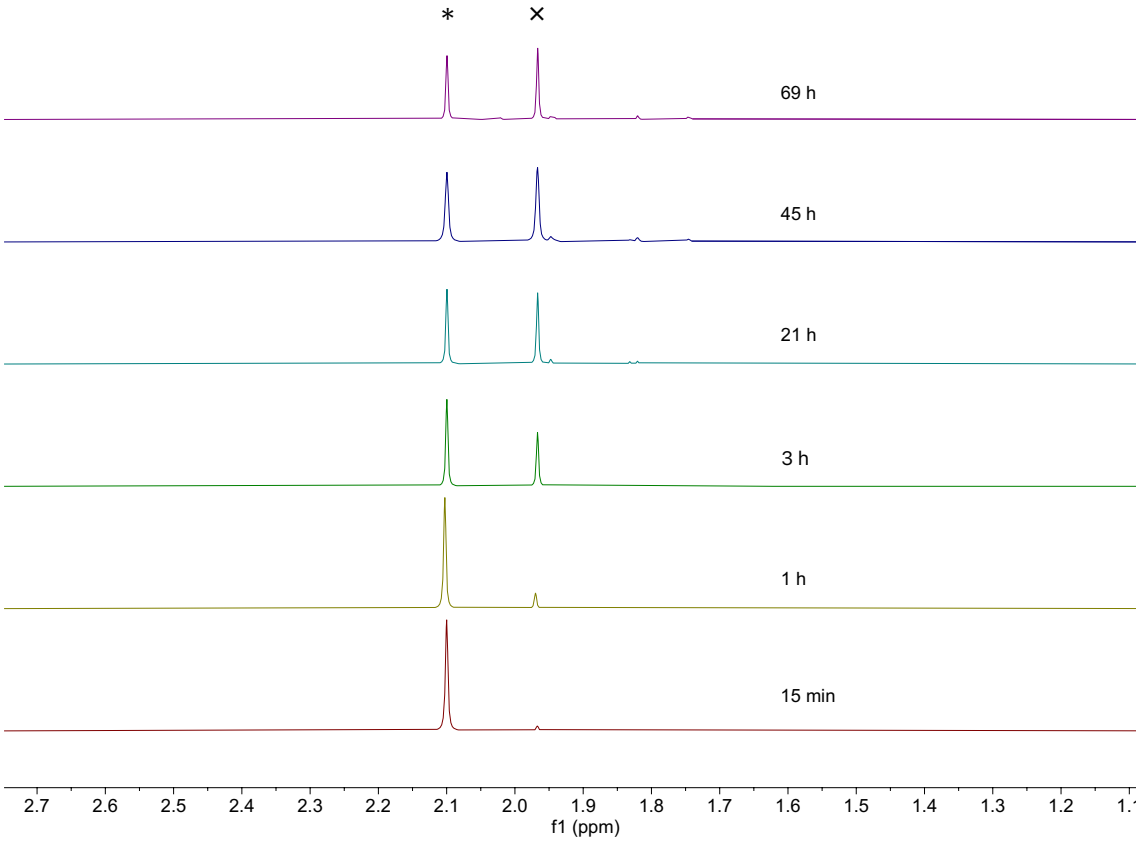

Figure S12. Expanded methyl region of ^{1}H NMR spectra of reaction between **1** and Ph_3PAu-C≡C-*p*-tol in C_6D_6 (∗2.10 ppm, ×1.97 ppm)

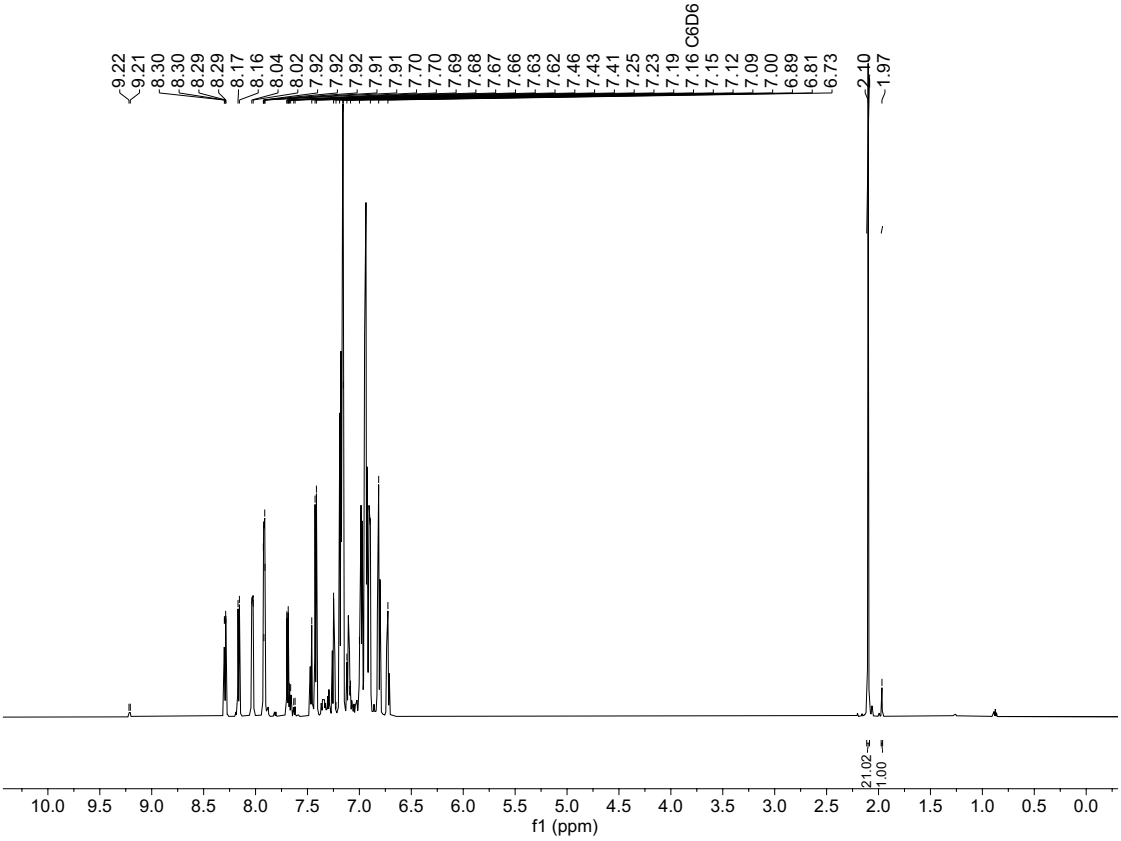

Figure S13. ^{1}H NMR spectrum of reaction between **1** and Ph_3PAu-C≡C-*p*-tol in C_6D_6 at 15 min.

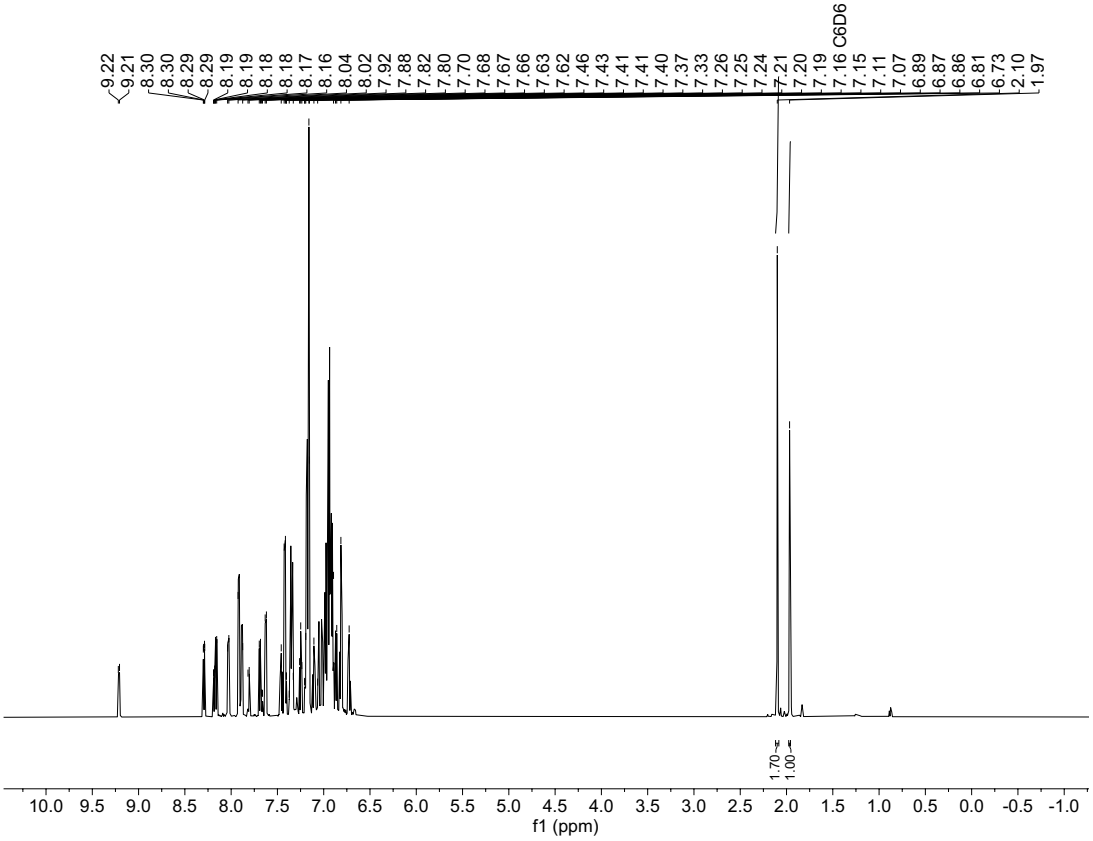

Figure S14. ^{1}H NMR spectrum of reaction between **1** and Ph_3PAu-C≡C-*p*-tol in C_6D_6 at 3 h.

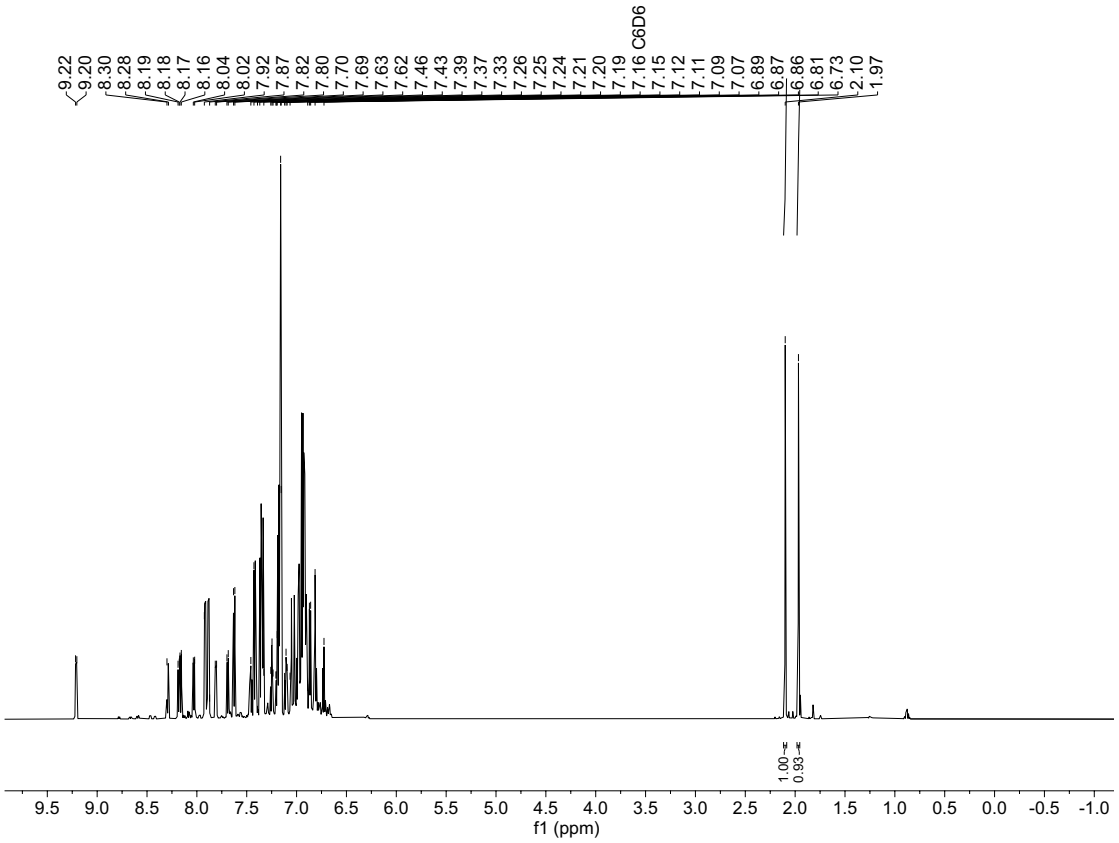

Figure S15. ^{1}H NMR spectrum of reaction between **1** and Ph_3PAu-C≡C-*p*-tol in C_6D_6 at 21 h

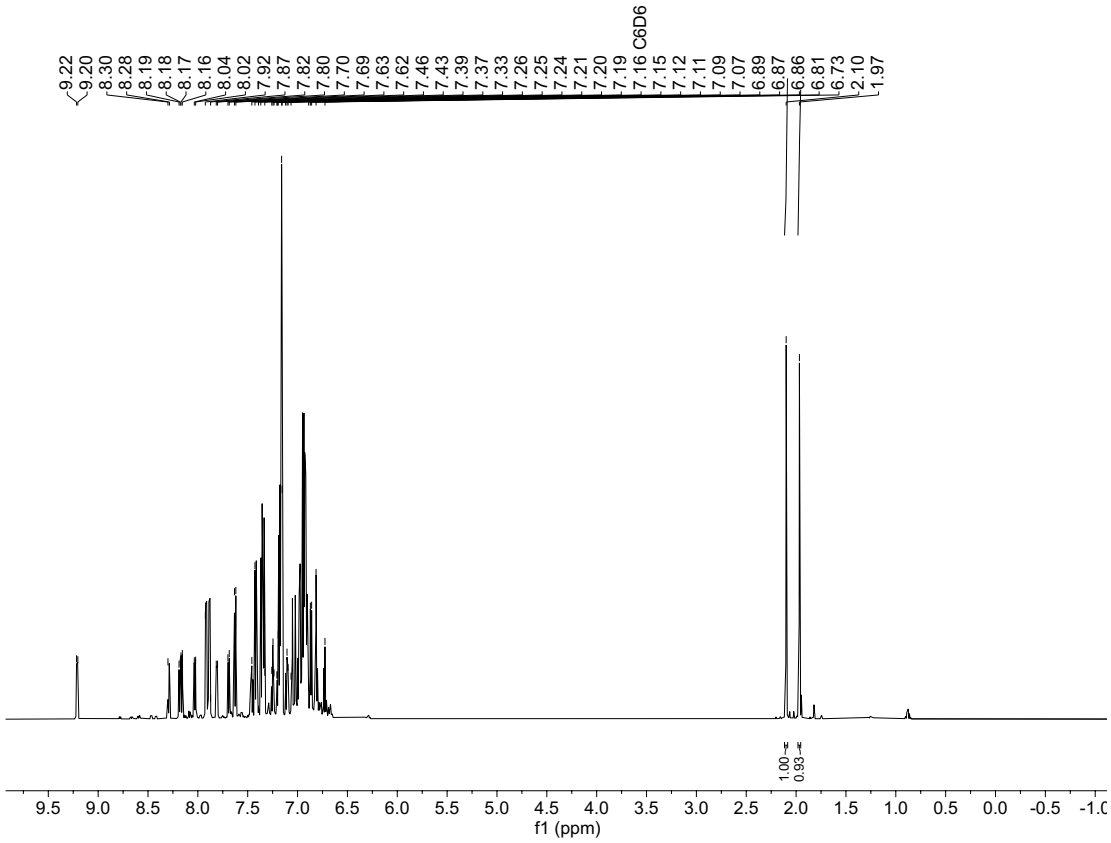

Figure S16. ^{1}H NMR spectrum of reaction between **1** and Ph_3PAu-C≡C-*p*-tol in C_6D_6 at 45 h.

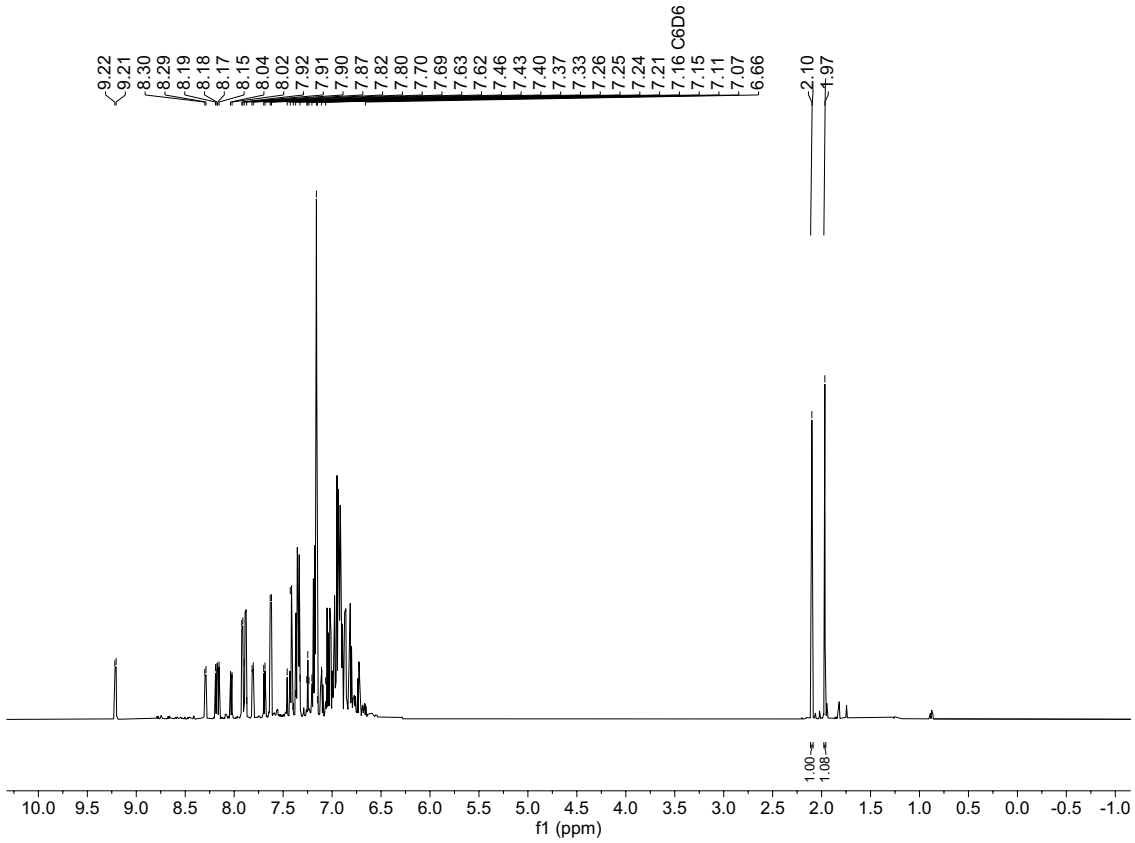

Figure S17. ^{1}H NMR spectrum of reaction between **1** and Ph_3PAu-C≡C-*p*-tol in C_6D_6 at 69 h.

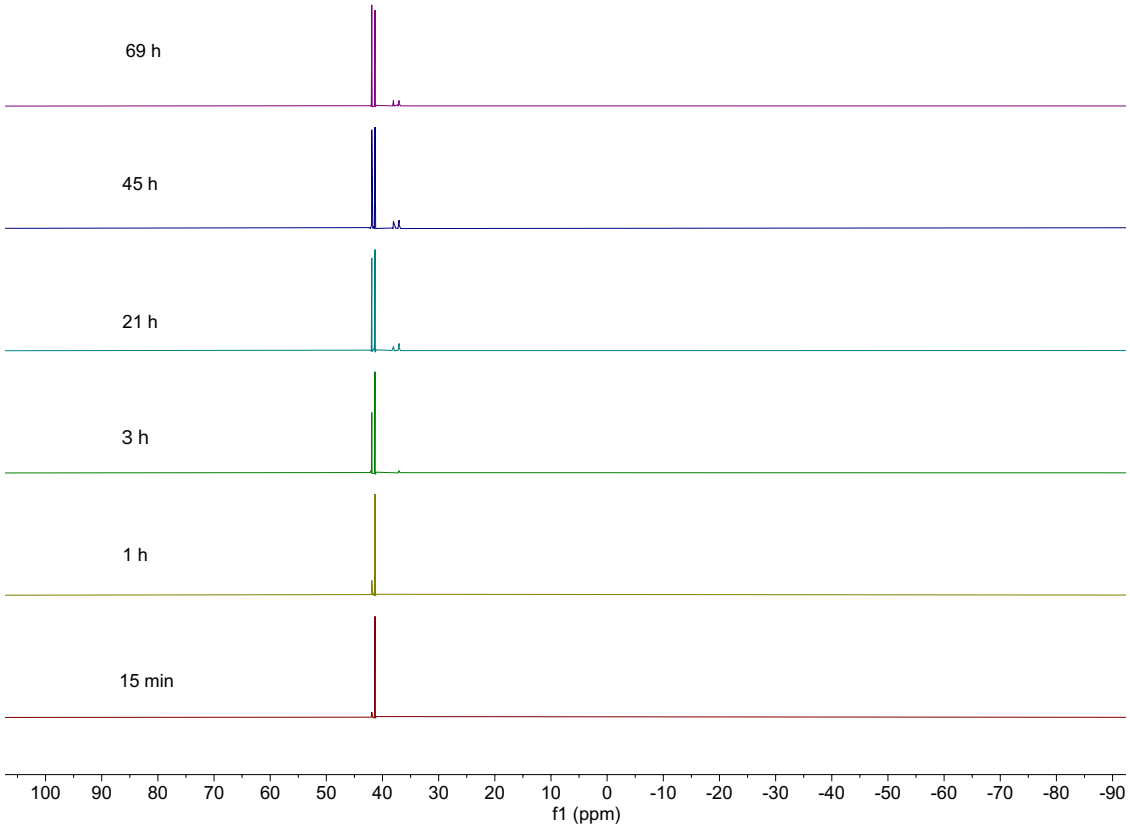

Figure S18. $^{31}P\ \{^{1}H\}$ NMR spectra of reaction between **1** and Ph_3PAu-C≡C-*p*-tol in C_6D_6

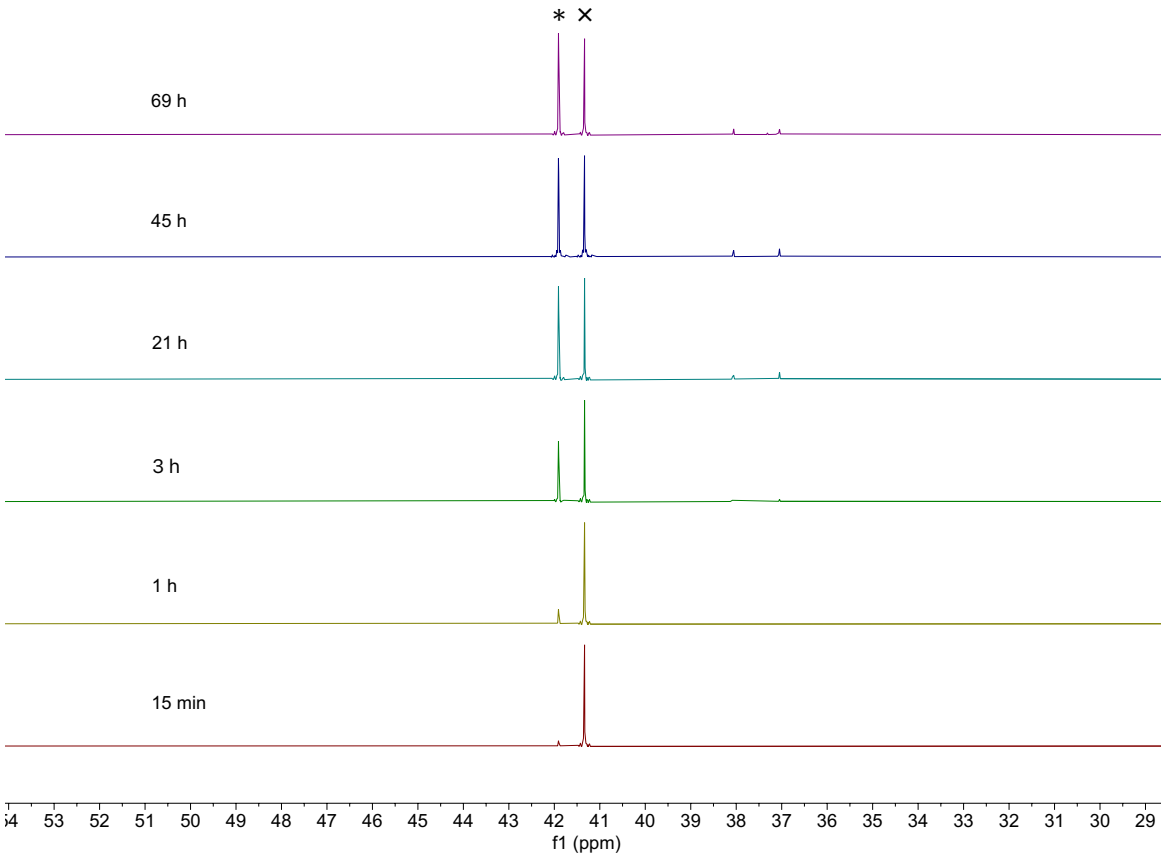

Figure S19. Expanded $^{31}P\ \{^{1}H\}$ NMR spectra of reaction between **1** and Ph_3PAu-C≡C-*p*-tol in C_6D_6 (∗41.9 ppm, ×41.3 ppm)

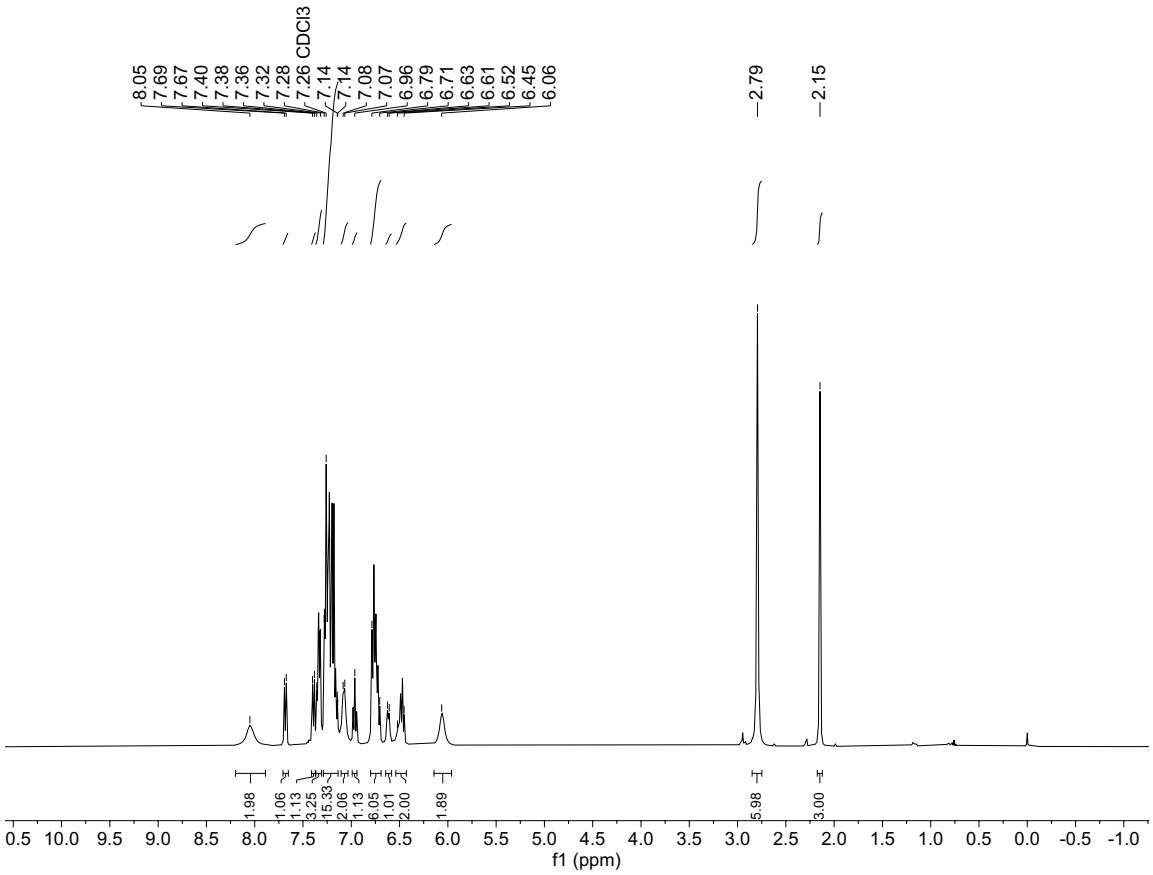

Figure S20. ^{1}H NMR spectrum of **3Z·DMAP** in $CDCl_3$.

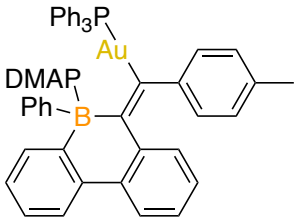

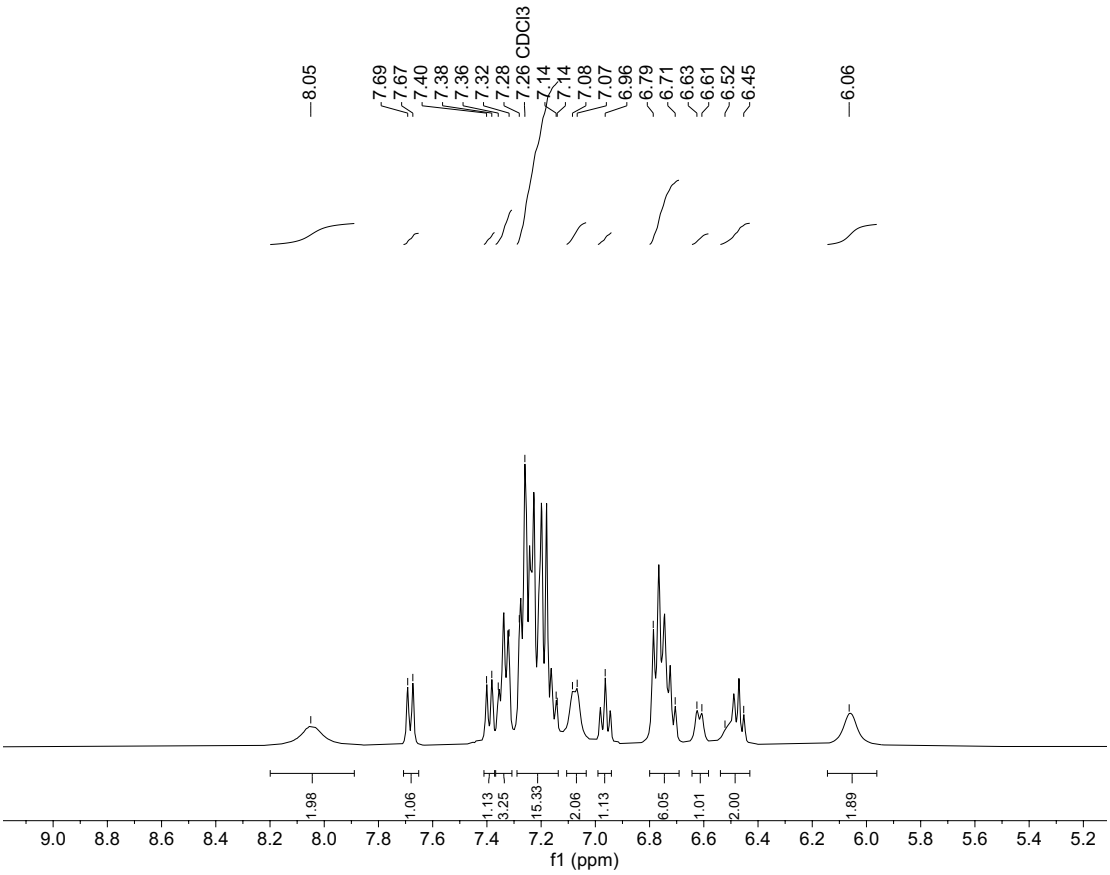

Figure S21. Expanded aryl region of ^{1}H NMR spectrum of **3Z·DMAP** in $CDCl_3$.

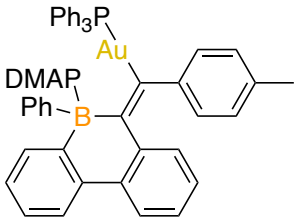

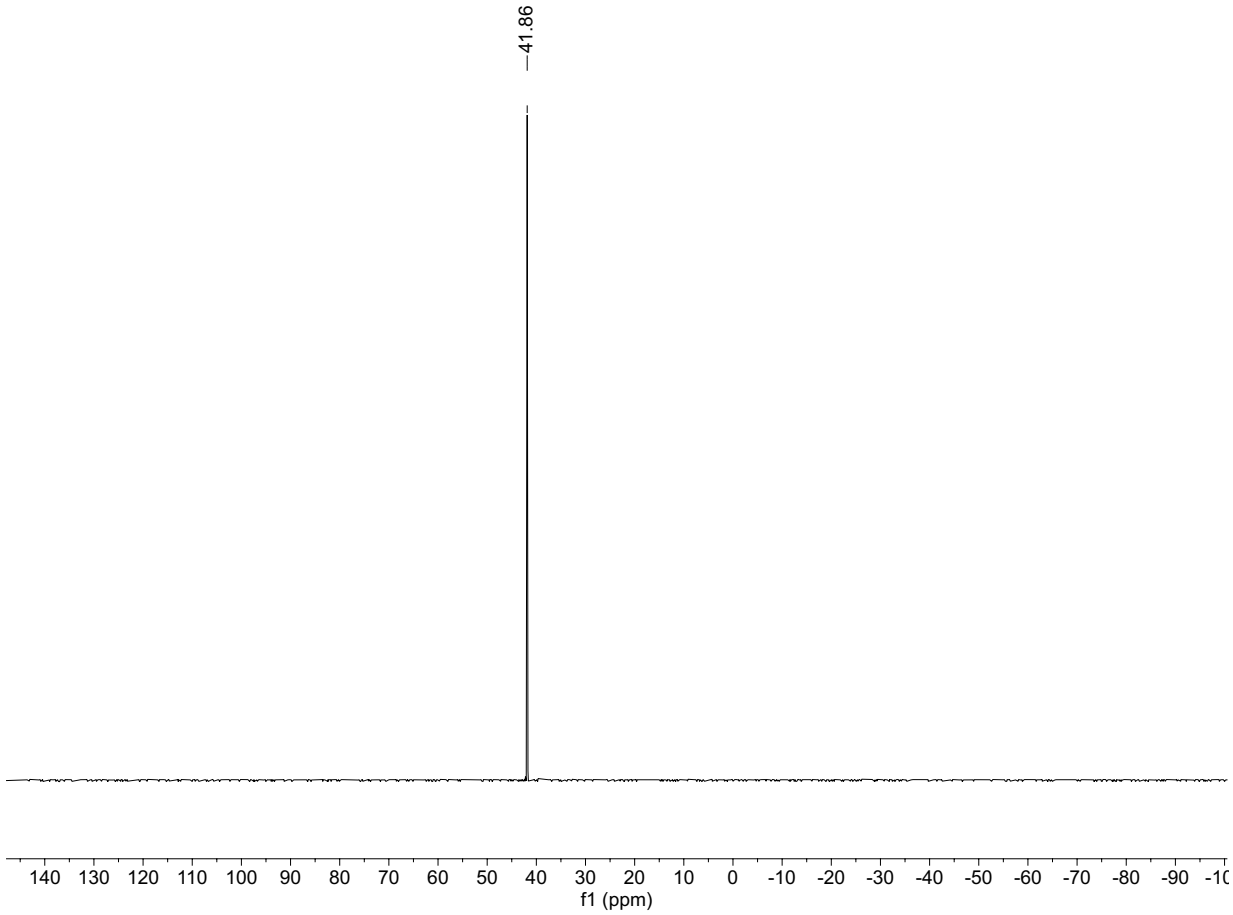

Figure S22. $^{31}P\{^{1}H\}$ spectrum of **3Z·DMAP** in C_6D_6.

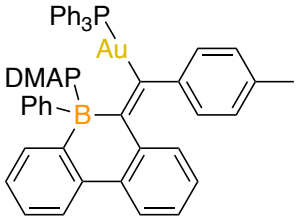

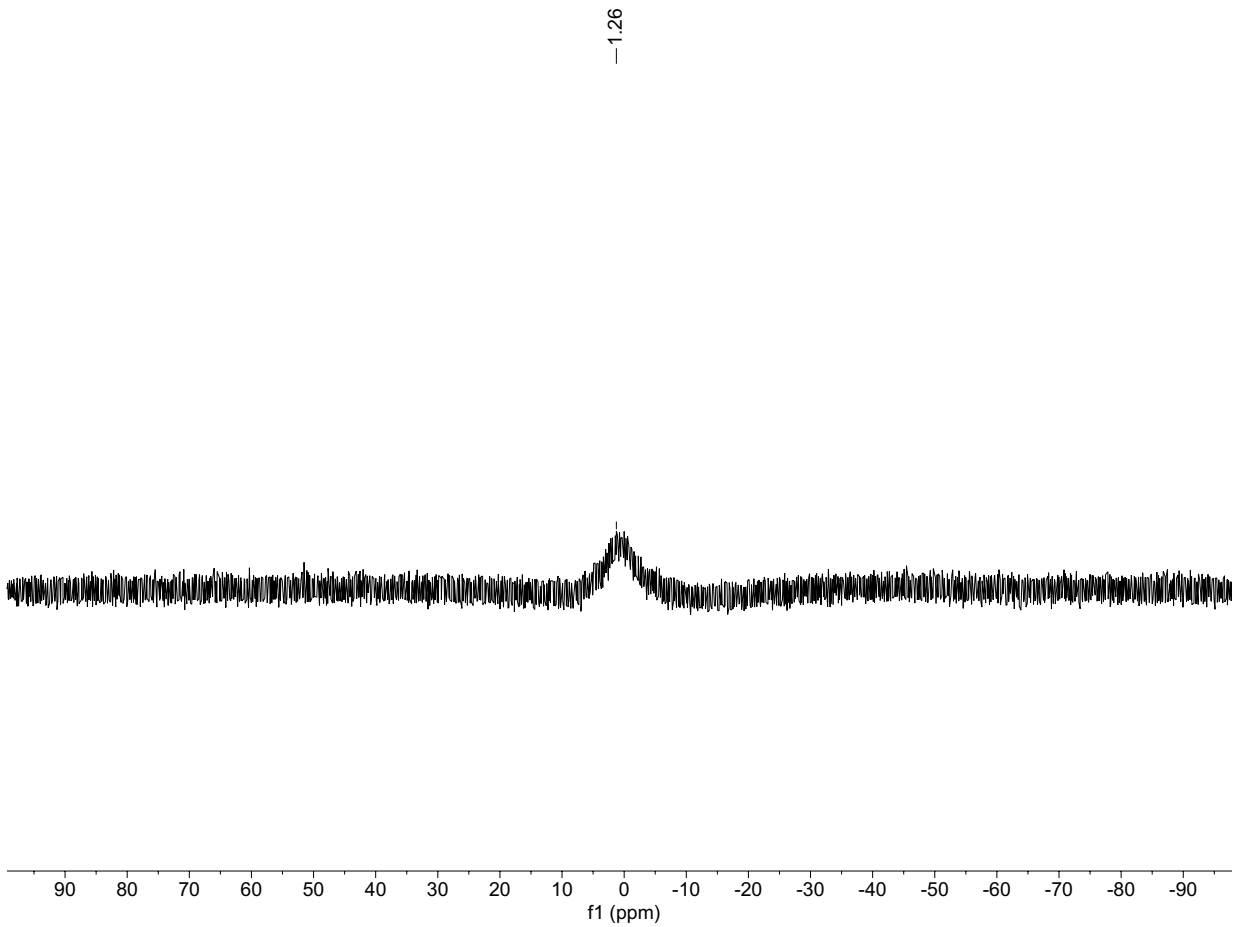

Figure S23. $^{11}B\{^{1}H\}$ spectrum of **3Z·DMAP** in C_6D_6.

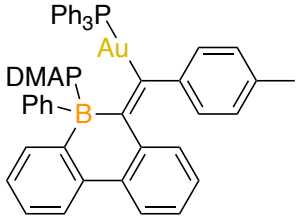

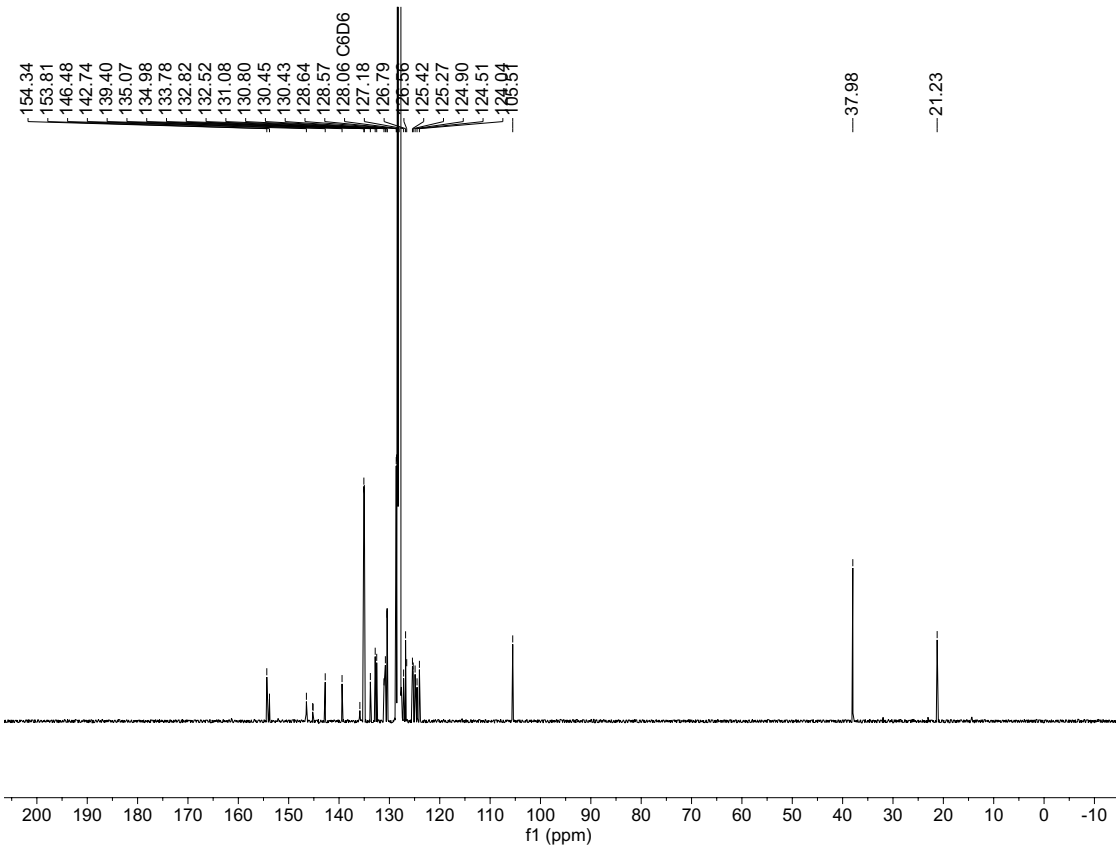

Figure S24. $^{13}C\{^{1}H\}$ NMR spectrum of **3Z·DMAP** in C_6D_6.

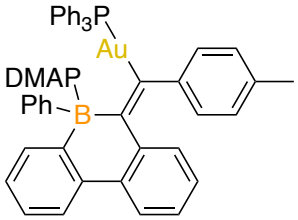

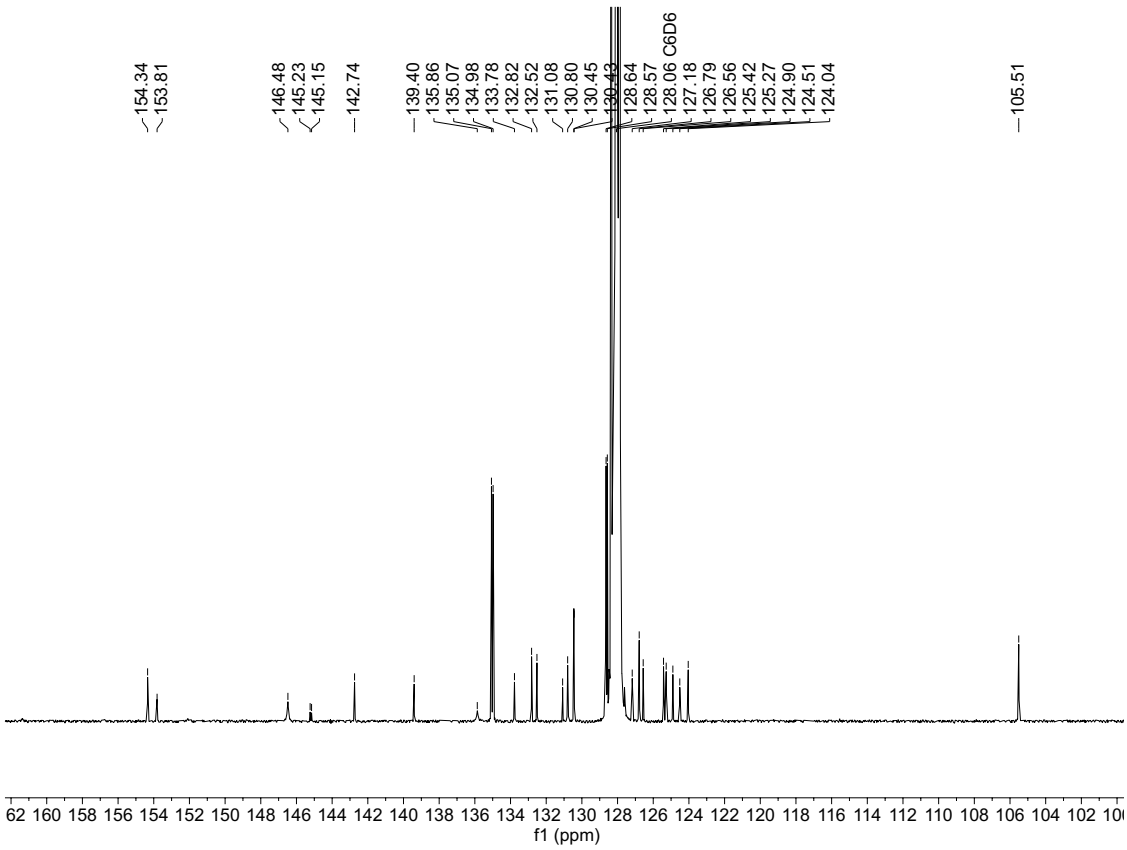

Figure S25. Expanded aryl region of $^{13}C\{^{1}H\}$ NMR spectrum of **3Z·DMAP** in C_6D_6.

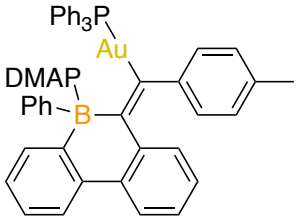

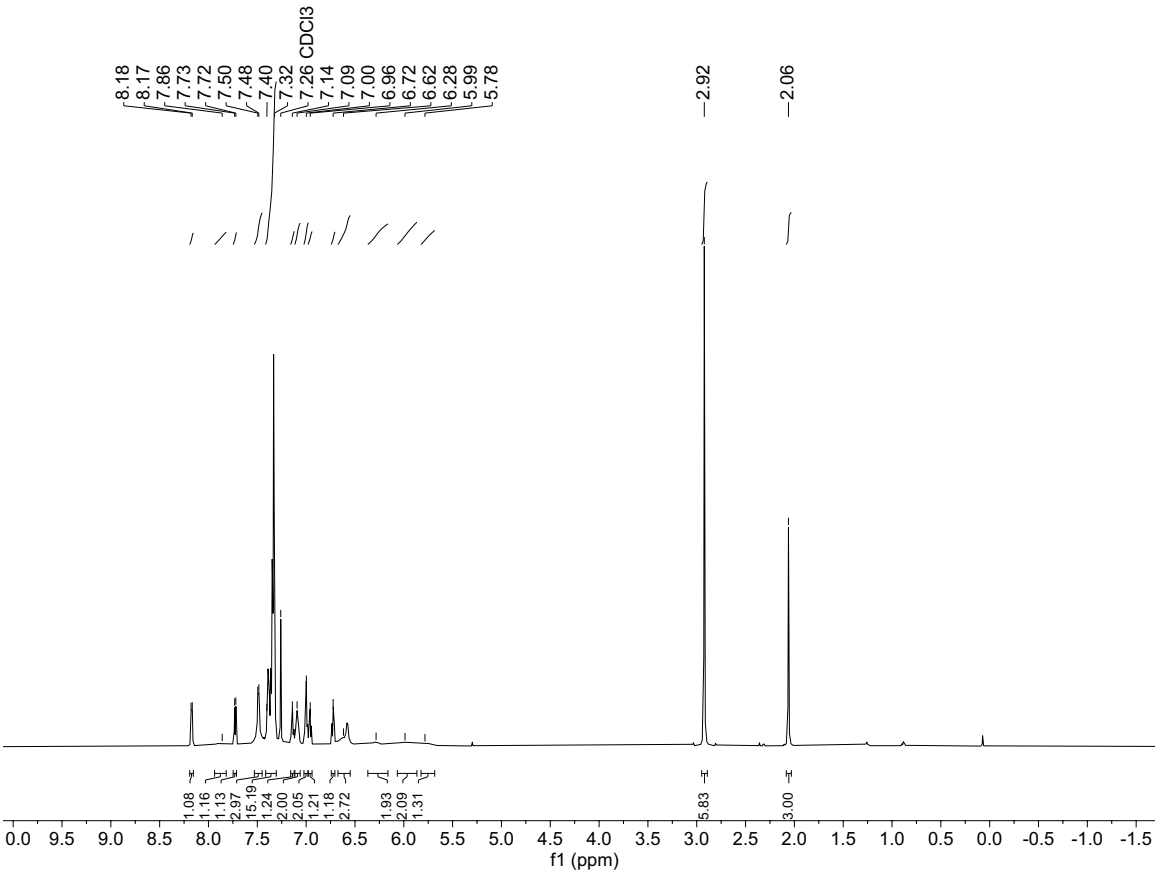

Figure S26. ^{1}H NMR spectrum of **3E·DMAP** in $CDCl_3$.

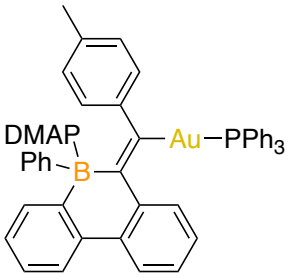

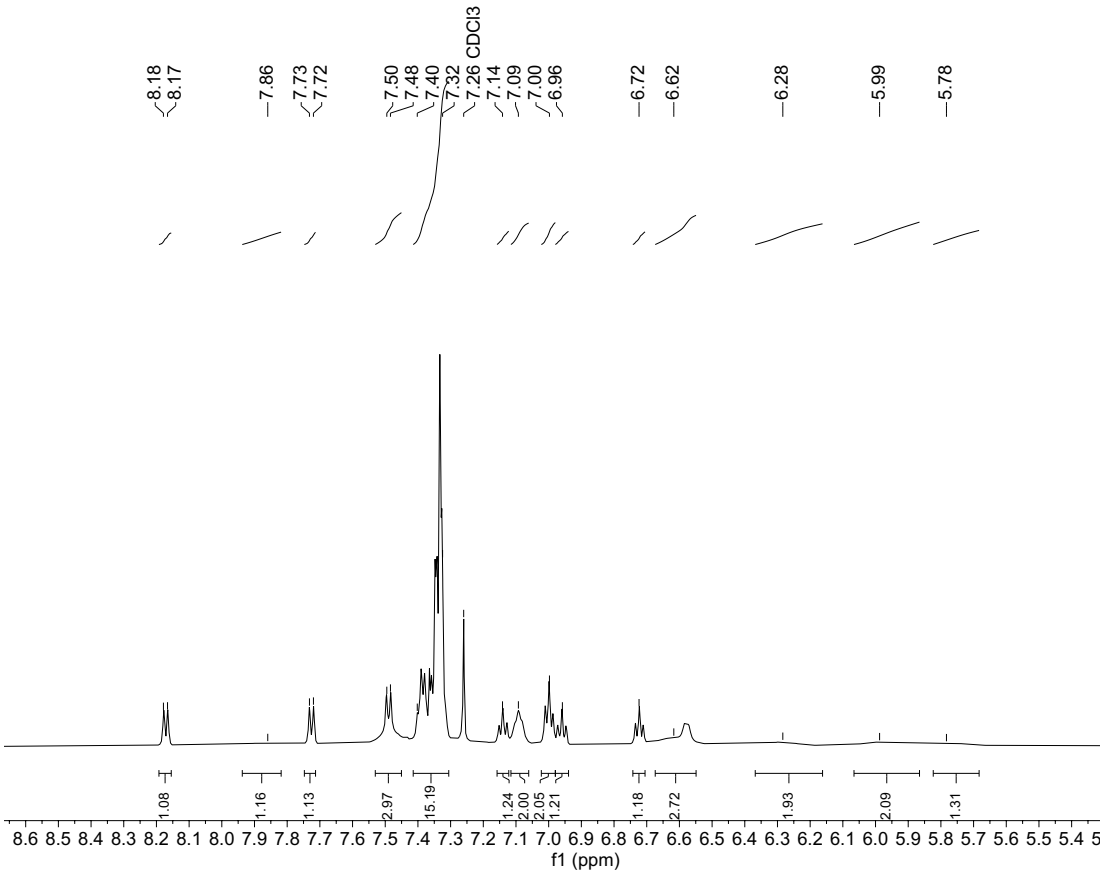

Figure S27. Expanded aryl region of ^{1}H NMR spectrum of **3E·DMAP** in $CDCl_3$.

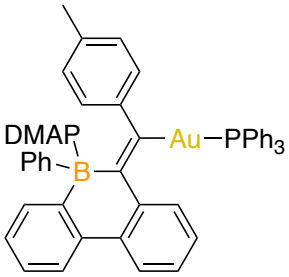

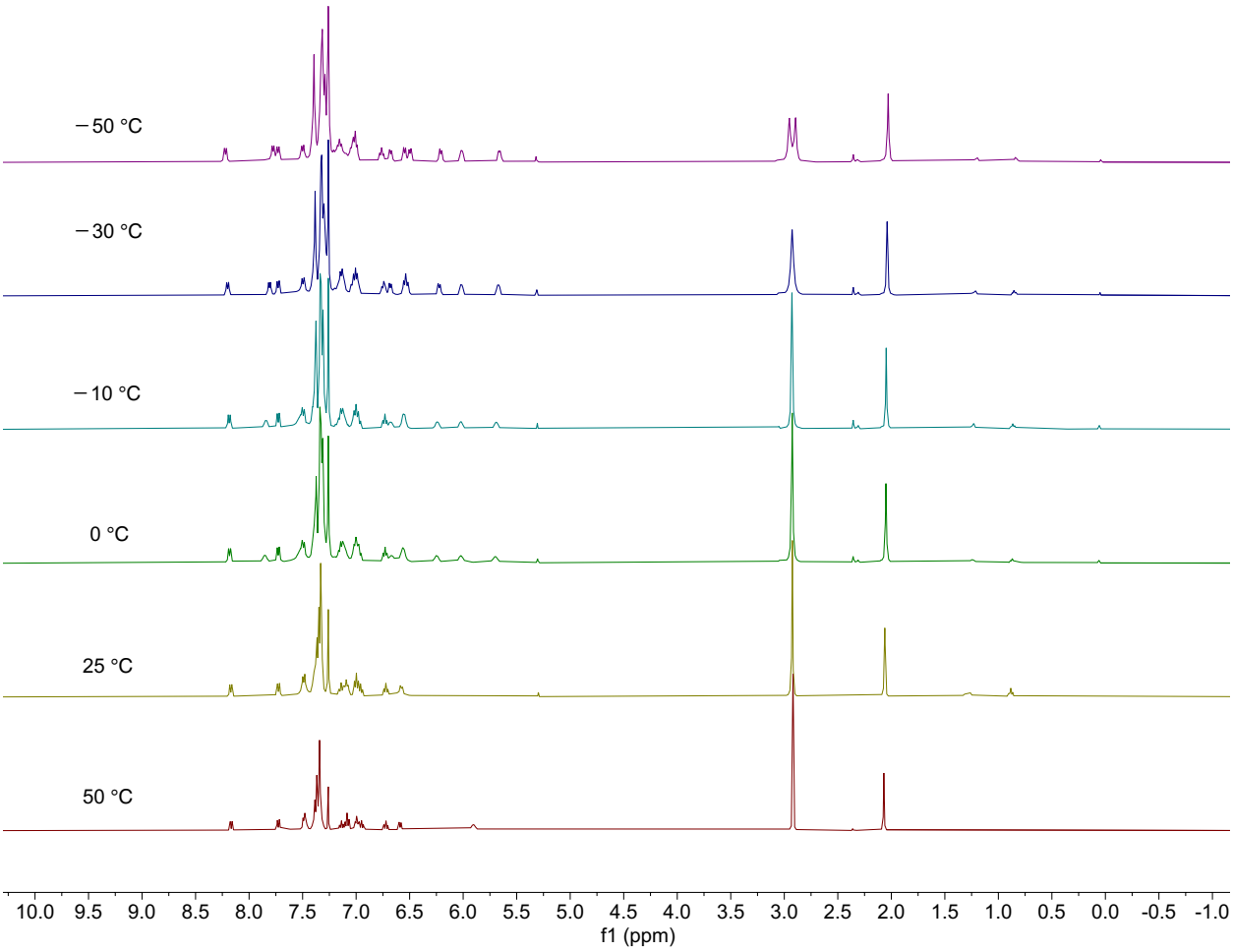

Figure S28. VT ^{1}H NMR spectra of **3E·DMAP** in $CDCl_3$.

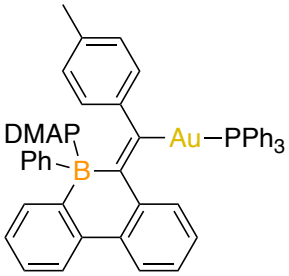

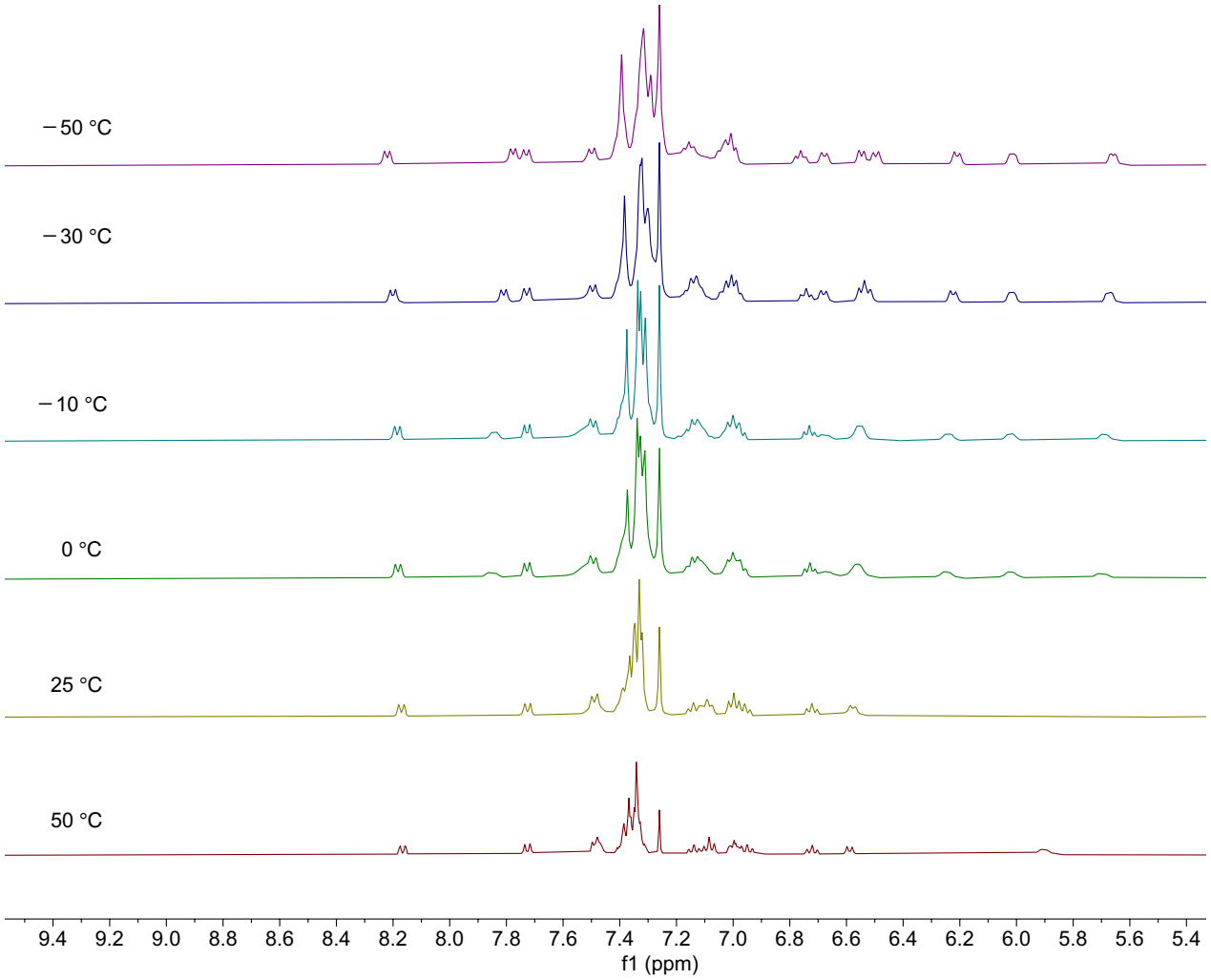

Figure S29. Expanded aryl region of VT ^{1}H NMR spectra of **3E·DMAP** in $CDCl_3$.

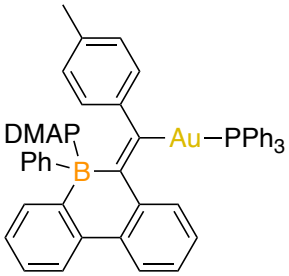

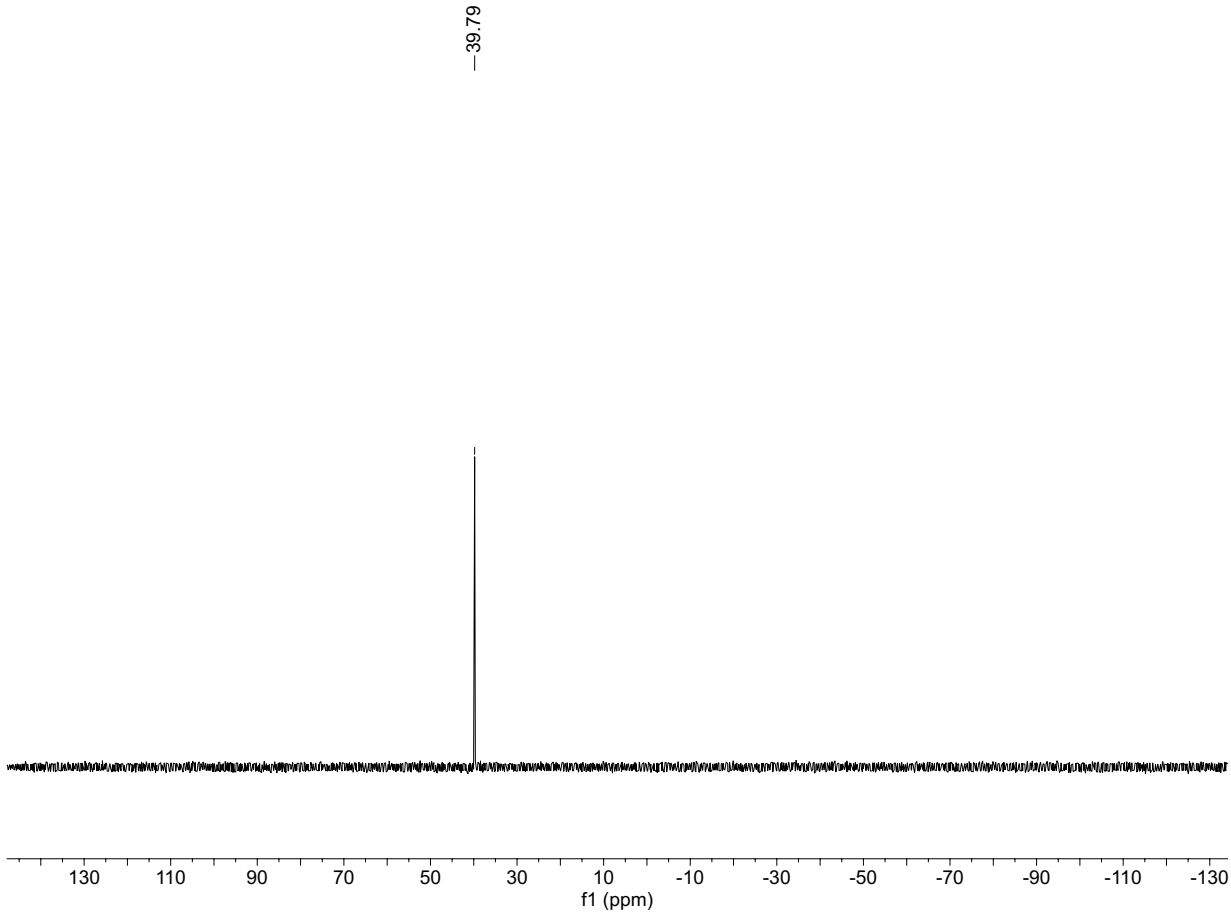

Figure S30. $^{31}P\{^{1}H\}$ spectrum of **3E·DMAP** in $CDCl_3$.

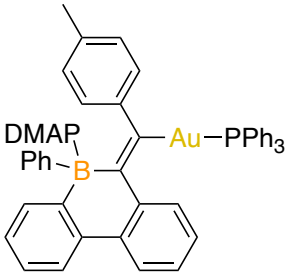

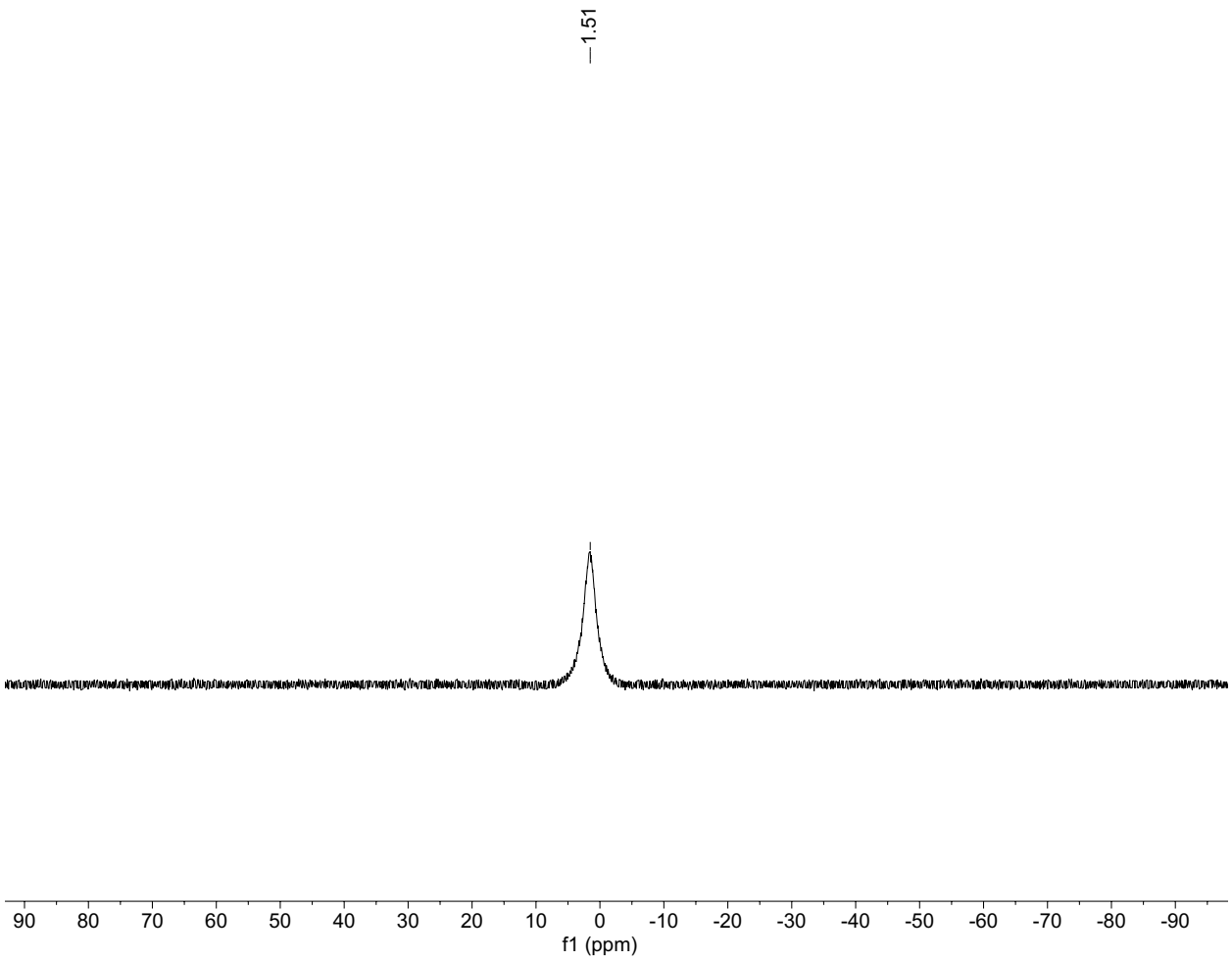

Figure S31. ^{11}B{1H} spectrum of **3E·DMAP** in $CDCl_3$.

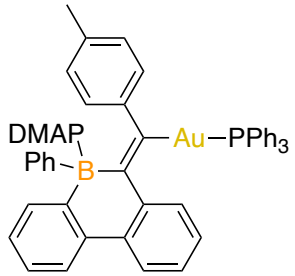

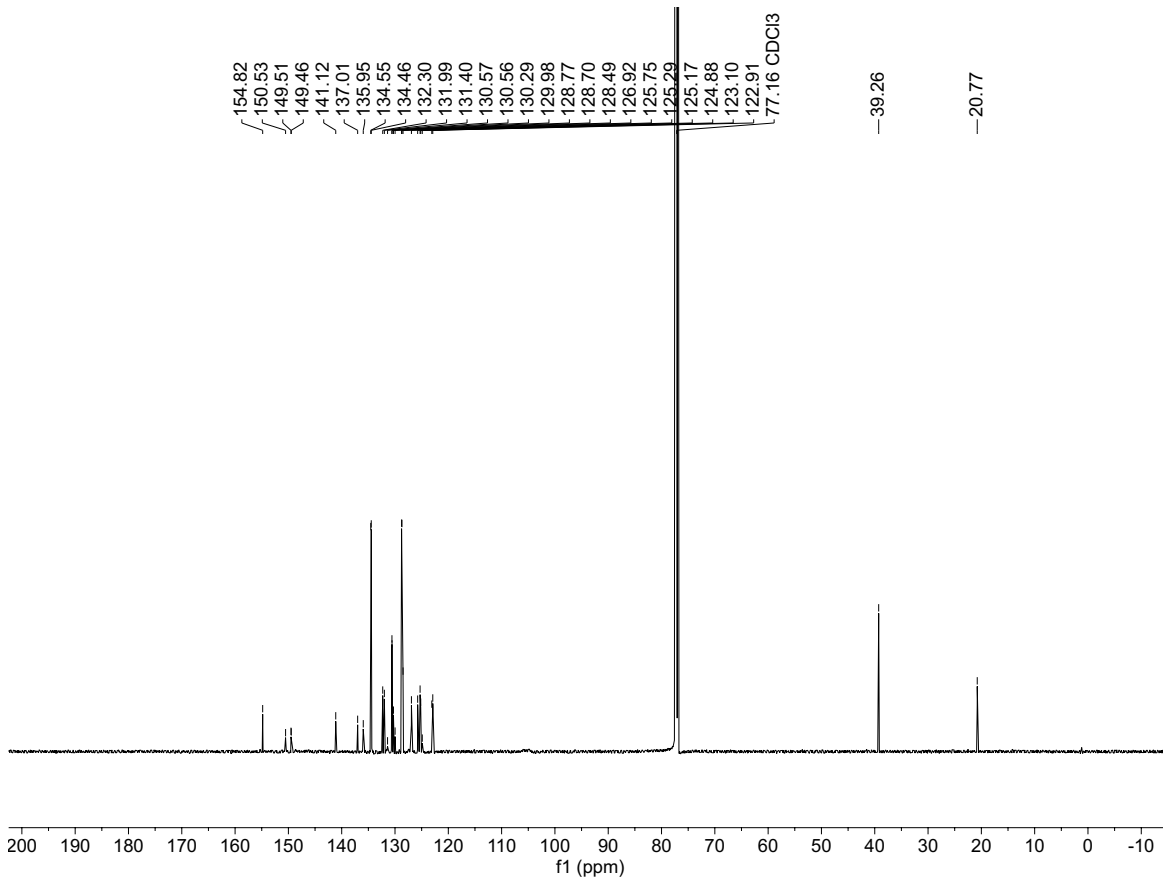

Figure S32. $^{13}C\{1H\}$ NMR spectrum of **3E·DMAP** in $CDCl_3$

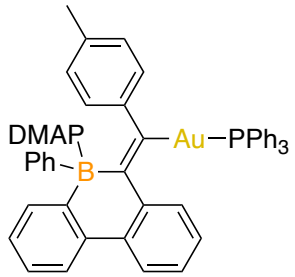

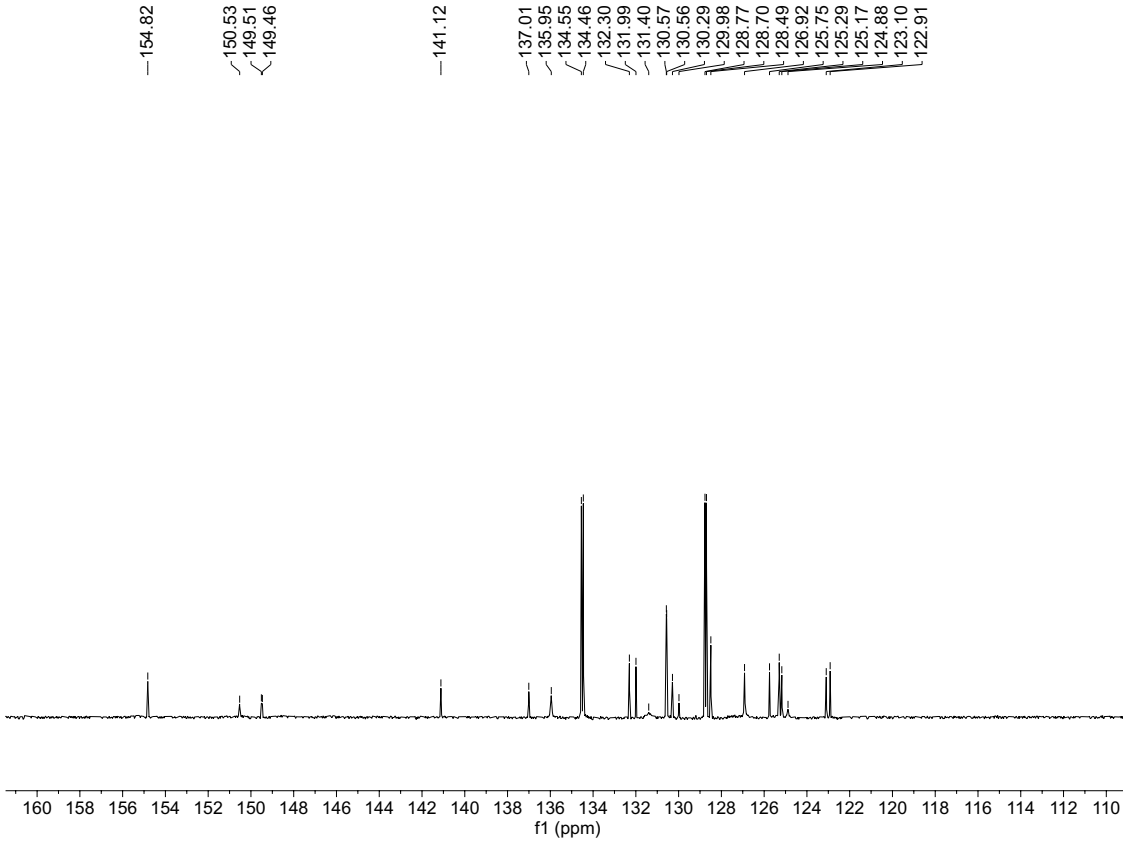

Figure S33. Expanded aryl region of $^{13}C\{^{1}H\}$ NMR spectrum of **3E·DMAP** in $CDCl_3$

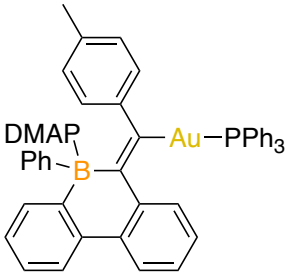

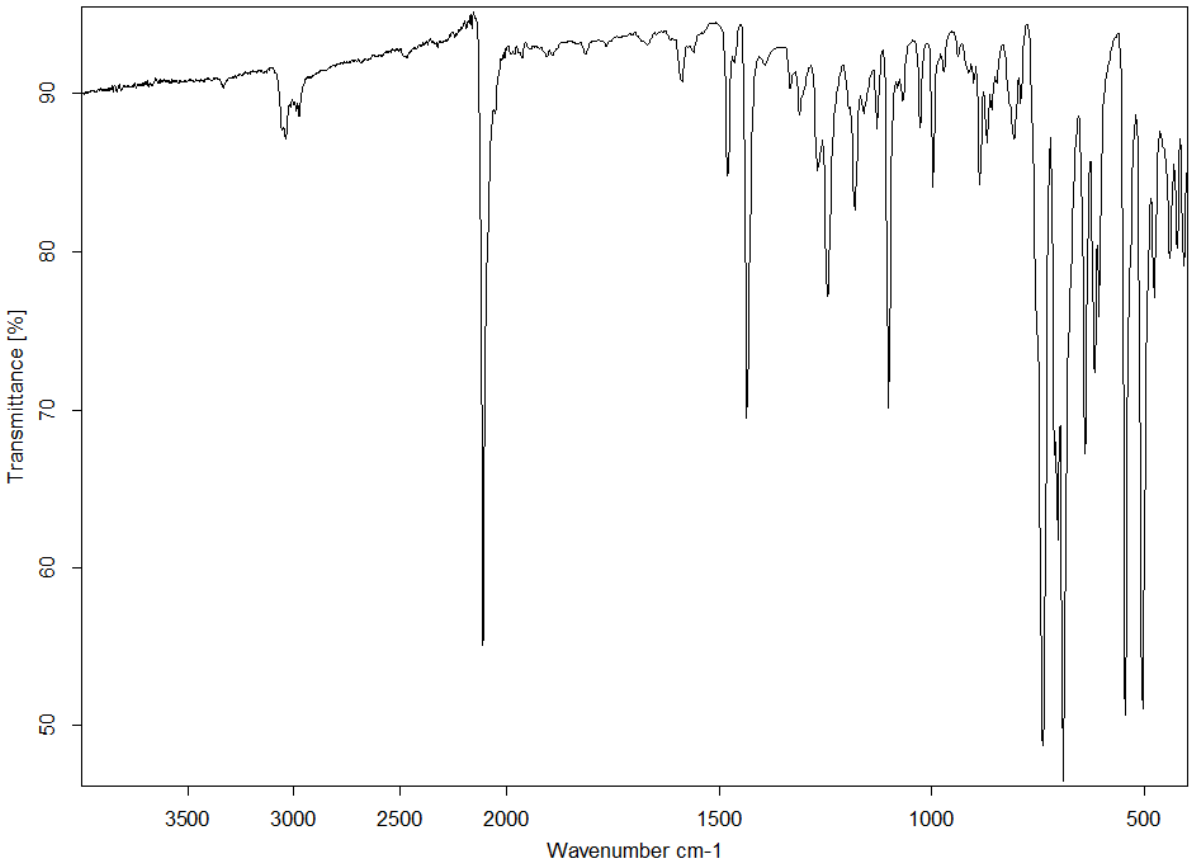

Figure S34. FT-IR spectrum of **2**.

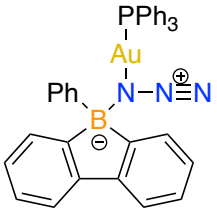

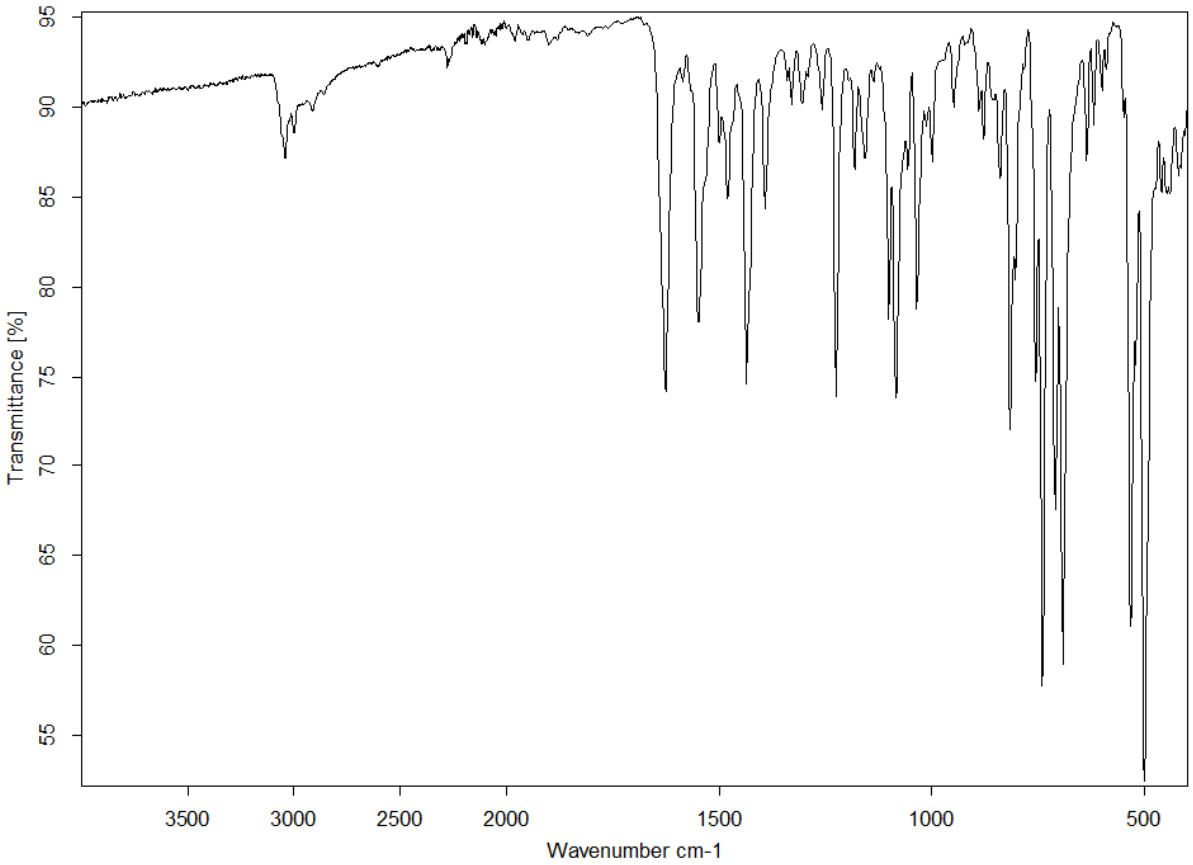

Figure S35. FT-IR spectrum of **3Z·DMAP**.

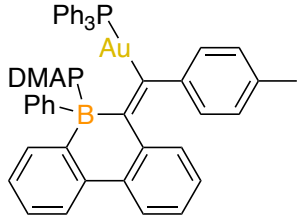

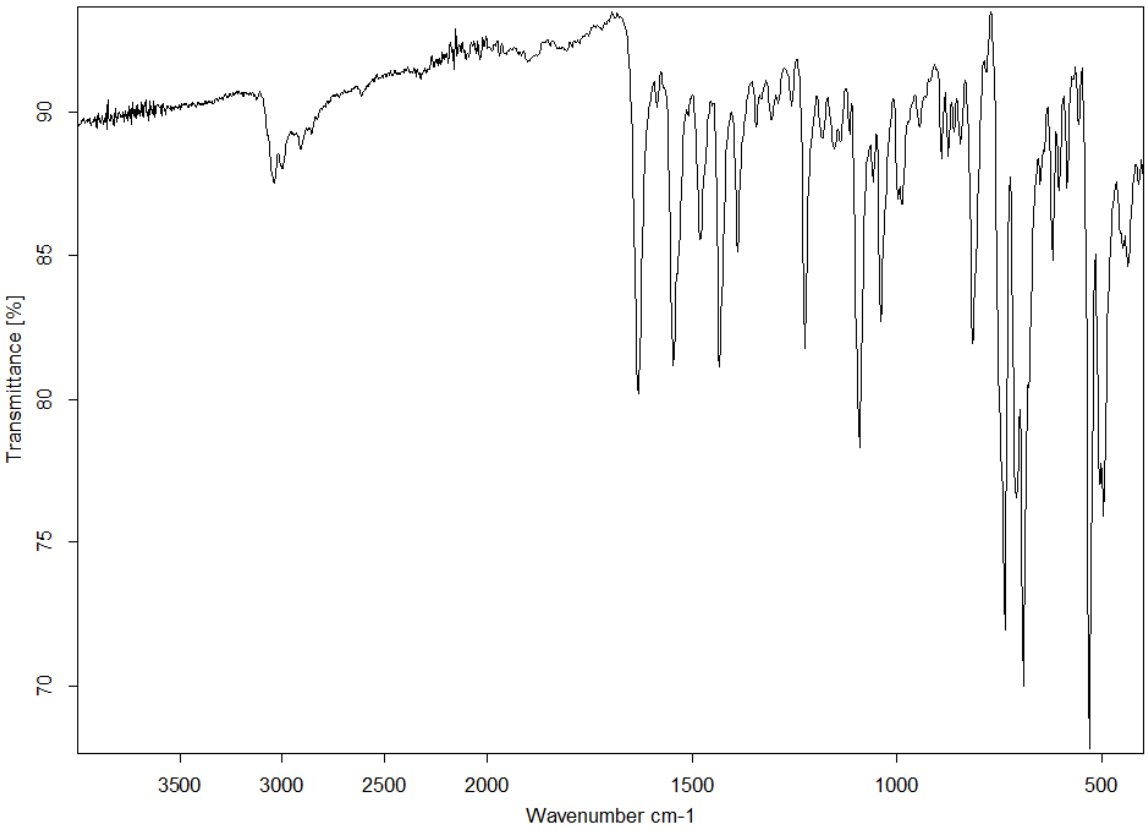

Figure S36. FT-IR spectrum of **3E·DMAP**.

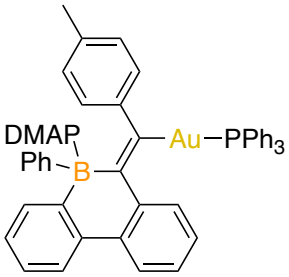

Table S1: X-ray crystallographic details for **2**, **3Z·DMAP**, **3E·DMAP**

	2	**3Z·DMAP**	**3E·DMAP**
CCDC	2219219	2219220	2219221
Empirical Formula	$C_{36}H_{28}AuBN_3P$	$C_{53}H_{47}BCl_2N_2P$	$C_{55}H_{52}AuBN_2P$
FW (g/mol)	741.36	1021.57	979.73
Crystal System	triclinic	triclinic	monoclinic
Space Group	P –1	P –1	$P\ 2_1/n$
a (Å)	10.2446(9)	12.804(2)	18.0377(5)
b (Å)	12.5326(9)	14.327(2)	18.2628(5)
c (Å)	12.8125(11)	14.901(3)	18.6944(5)
$\boldsymbol{\alpha}$ (°)	75.113(3)	82.115(7)	90
$\boldsymbol{\beta}$ (°)	80.036(3)	82.921(7)	118.3750(10)
$\boldsymbol{\gamma}$ (°)	67.918(2)	76.566(7)	90
V (Å^3)	1467.8(2)	2621.7(8)	5418.4(3)
Z	2	2	4
D_c (g cm^{-3})	1.677	1.294	1.201
Radiation $\boldsymbol{\lambda}$ (Å)	0.71073	0.71073	0.71073
Temp (K)	150	150	150
R1 [I>2($\boldsymbol{\sigma}$)I][a]	0.0599	0.0456	0.0180
wR2 (F^2)[a]	0.1612	0.1071	0.0469
GOF (S)[a]	1.078	1.068	1.053

[a] $R1(F[I > 2(I)]) = \sum||F_o| - |F_c||/ \sum |F_o|$; $wR2(F^2\,[\text{all data}]) = \{[w(F_o^2 - F_c^2)2]/[w(F_o^2)^2]\}^{1/2}$; $S(\text{all data}) = [w(F_o^2 - F_c^2)^2/(n - p)]^{1/2}$ (n = no. of data; p = no. of parameters varied; $w = 1/\sigma^2(F_o^2) + (aP)^2 + bP$] where $P = (F_o^2 + 2F_c^2)/3$ and a and b are constants suggested by the refinement program.

5. Computational Details

Geometries were fully optimized using the Gaussian 16 software package[1] and visualized using GaussView 6.[2] All relevant minima and transition states were fully optimized in the gas phase at the B3LYP[3,4] level of theory employing correlation-consistent polarized valence double-ζ Dunning (DZ) basis sets with cc-pVDZ quality[5,6] from the EMSL basis set exchange library, using a small core pseudopotential on all metals.[7] All calculations were performed using standard Gaussian 16 SCF convergence criteria with the density fitting approximation (Resolution of Identity, RI)[8–11]. The nature of each stationary point was checked with an analytical second-derivative calculation (no imaginary frequency for minima). Final single-point energies were calculated by employing triple-ζ Dunning (TZ) basis sets (cc-pVTZ quality)[5] while retaining the B3LYP functional. Solvent effects (benzene, $\varepsilon = 2.27$) with the Solvent Model based on Density (SMD) were included in the single point calculations.[12] Grimme dispersion corrections with zero damping (keyword -zero) were added at this stage using the standalone dftd3 program.[13] Enthalpies and Gibbs free energies were then obtained from TZ single-point energies and thermal corrections from the B3LYP/cc-pVDZ-(PP) vibrational analyses (at 298 K and 1 atm); entropy corrections were scaled by a factor of 0.67 to account for decreased entropy in the condensed phase.[14–16]

5.1. Comparison between X-ray and Calculated Structures

Table S2. Comparison between the X-ray structures (Exp) and calculated structure (DFT) of **2** optimized at B3LYP/cc-pVDZ level of theory.

Bond Parameters	**2** (Exp)	**2** (DFT)	% Error
Au(1)－N(1) (Å)	2.07	2.09	1
B(1)－N(1) (Å)	1.65	1.70	3
N(1)－N(2) (Å)	1.23	1.24	1
N(2)－N(3) (Å)	1.12	1.14	2
∠P(1)-Au(1)-N(1) (°)	171.6	177.4	3
∠N(1)-N(2)-N(3) (°)	177.8	178.0	0

Table S3. Comparison between the X-ray structure (Exp) and calculated structure (DFT) of **3Z·DMAP** optimized at B3LYP/cc-pVDZ level of theory.

Bond Parameters	**3Z·DMAP** (Exp)	**3Z·DMAP** (DFT)	% Error
Au(1)－C(7) (Å)	2.05	2.08	1
C(7)=C(6) (Å)	1.37	1.37	0
B(1)－C(6) (Å)	1.62	1.63	1
B(1)－N(1) (Å)	1.63	1.65	1
∠Au(1)-C(7)-C(6) (°)	122.1	125.8	3

Table S4. Comparison between the X-ray structure (Exp) and calculated structure (DFT) of **3E·DMAP** optimized at B3LYP/cc-pVDZ level of theory.

Bond Parameters	**3E·DMAP** (Exp)	**3E·DMAP** (DFT)	% Error
Au(1)－C(7) (Å)	2.06	2.09	1
C(7)=C(6) (Å)	1.36	1.37	1
B(1)－C(6) (Å)	1.62	1.64	1
B(1)－N(1) (Å)	1.61	1.64	2
∠Au(1)-C(7)-C(6) (°)	123.5	121.6	-2

5.2. Energy Tables

Table S5. Final Energies, Enthalpy and Entropy Corrections, Gibbs Free Energies from B3LYP functional with Zero Damping Dispersion Correction-D0. In Hartree. See Computational Details for Methods.

Compound	E(B3LYP/cc-pVDZ)	E(B3LYP(SMD)/cc-pVTZ)	ZPE	D0	$H_{correction}$	$G_{correction}$	$S_{correction}$	G
DMAP	-382.275064	-382.402879	0.160879	-0.012919	0.170503	0.126976	0.043527	-382.274458
1	-718.652565	-718.882321	0.255096	-0.027167	0.269909	0.213603	0.056306	-718.677304
PPh_3AuN_3 + 1	-1336.400823	-1336.627650	0.287269	-0.043820	0.309903	0.229546	0.080357	-1336.415406
2	-2055.084980	-2055.577618	0.543018	-0.096462	0.581021	0.465199	0.115822	-2055.170660
2g	-2055.078674	-2055.573881	0.543032	-0.085655	0.581097	0.462257	0.118840	-2055.158062
Ph_3PAu-C≡C-*p*-tol	-1519.331460	-1519.680558	0.401388	-0.054033	0.429116	0.336821	0.092295	-1519.367312
3E·DMAP	-2620.325736	-2620.996177	0.822982	-0.144207	0.875785	0.726842	0.148943	-2620.364391
3E	-2238.033699	-2238.582152	0.659393	-0.106838	0.702586	0.574723	0.127863	-2238.072072
3Z·DMAP	-2620.320760	-2620.992101	0.822891	-0.150987	0.875805	0.726789	0.149016	-2620.367123
3Z	-2237.376343	-2238.579528	0.659415	-0.109629	0.702706	0.573651	0.129055	-2238.072917

Table S6. Final Energies, Enthalpy and Entropy Corrections, Gibbs Free Energies from B3LYP functional with Zero Damping Dispersion Correction-D0. In Hartree. See Computational Details for Methods.

Compound	E(B3LYP/cc-pVDZ)	E(B3LYP(SMD)/cc-pVTZ)	ZPE	D0	$H_{correction}$	$G_{correction}$	$S_{correction}$	G
DMAP	-382.275064	-382.402879	0.160879	-0.012919	0.170503	0.126976	0.043527	-382.274458
1	-718.652565	-718.882321	0.255096	-0.027167	0.269909	0.213603	0.056306	-718.677304
HN_3 + 1	-164.798116	-164.847465	0.021337	-0.000440	0.025502	-0.001666	0.027168	-164.798116
H-2	-883.4689488	-883.728839	0.278077	-0.037114	0.297163	0.230426	0.066737	-883.513504
H-C≡C-*p*-tol+1	-347.731699	-347.846277	0.136251	-0.009833	0.145545	0.102195	0.043350	-347.739610
H-3E·DMAP	-1448.761599	-1449.202843	0.560221	-0.084691	0.593235	0.494488	0.098747	-1448.760459
H-3E	-1066.463875	-1066.781760	0.396364	-0.050070	0.419797	0.342213	0.077584	-1066.464014
H-3Z·DMAP	-1448.763642	-1449.206233	0.560079	-0.079779	0.593224	0.493374	0.099850	-1448.759687
H-3Z	-1066.461900	-1066.779445	0.396765	-0.048998	0.420137	0.342828	0.077309	-1066.460103

5.3. Relative Enthalpies and Gibbs Free Energies

Table S7. Relative Energies (zero damping corrections, B3LYP/SMD corrected SPE)- Bolded is energy reference structure. All values are in kcal/mol at 298 K and 1 atm.

Compound	ΔH	ΔG
PPh_3AuN_3 + **1**	**0.0**	**0.0**
2	-57.7	-48.9
2g	-48.5	-41.0
Ph_3PAu-C≡C-*p*-tol + **1**	**0.0**	**0.0**
3E·DMAP	-46.6	-28.4
3E	-25.9	-17.2
3Z·DMAP	-48.3	-30.2
3Z	-26.0	-17.8

Table S8. Relative Energies (zero damping corrections, B3LYP/SMD corrected SPE)- Bolded is energy reference structure. All values are in kcal/mol at 298 K and 1 atm.

Compound	ΔH	ΔG
HN_3 + **1**	**0.0**	**0.0**
H-2	-4.3	2.8
H-C≡C-*p*-tol + **1**	**0.0**	**0.0**
H-3E·DMAP	-62.0	-43.4
H-3E	-38.8	-29.6
H-3Z·DMAP	-61.1	-42.9
H-3Z	-36.5	-27.1

References

1. Frisch, M. J.; Trucks, G. W.; Schlegel, H. B.; Scuseria, G. E.; Robb, M. a.; Cheeseman, J. R.; Scalmani, G.; Barone, V.; Petersson, G. a.; Nakatsuji, H.; Li, X.; Caricato, M.; Marenich, a. V.; Bloino, J.; Janesko, B. G.; Gomperts, R.; Mennucci, B.; Hratchian, H. P.; Ortiz, J. V.; Izmaylov, a. F.; Sonnenberg, J. L.; Williams; Ding, F.; Lipparini, F.; Egidi, F.; Goings, J.; Peng, B.; Petrone, A.; Henderson, T.; Ranasinghe, D.; Zakrzewski, V. G.; Gao, J.; Rega, N.; Zheng, G.; Liang, W.; Hada, M.; Ehara, M.; Toyota, K.; Fukuda, R.; Hasegawa, J.; Ishida, M.; Nakajima, T.; Honda, Y.; Kitao, O.; Nakai, H.; Vreven, T.; Throssell, K.; Montgomery Jr., J. a.; Peralta, J. E.; Ogliaro, F.; Bearpark, M. J.; Heyd, J. J.; Brothers, E. N.; Kudin, K. N.; Staroverov, V. N.; Keith, T. a.; Kobayashi, R.; Normand, J.; Raghavachari, K.; Rendell, a. P.; Burant, J. C.; Iyengar, S. S.; Tomasi, J.; Cossi, M.; Millam, J. M.; Klene, M.; Adamo, C.; Cammi, R.; Ochterski, J. W.; Martin, R. L.; Morokuma, K.; Farkas, O.; Foresman, J. B.; Fox, D. J. Gaussian 16, Revision C.01. *Gaussian 16, Rev. C. 01. Gaussian Inc., Wallingford CT* **2016**.
2. Dennington, R.; Keith, T. A.; Millam, J. M. GaussView, Version 6.0. 16. *GaussView, Version 6. Semichem Inc. Shawnee Mission KS* **2016**.
3. A. D. Becke, *J. Chem. Phys.*, 1993, **98**, 5648-5652.
4. C. Lee, W. Yang and R. G. Parr, *Physical Review B*, 1988, **37**, 785-789.
5. N. B. Balabanov and K. A. Peterson, *J. Chem. Phys.*, 2005, **123**, 064107.
6. N. B. Balabanov and K. A. Peterson, *J. Chem. Phys.*, 2005, **123**, 064107.
7. K. L. Schuchardt, B. T. Didier, T. Elsethagen, L. Sun, V. Gurumoorthi, J. Chase, J. Li and T. L. Windus, *J. Chem. Inf. Model*, 2007, **47**, 1045-1052.
8. E. J. Baerends, D. E. Ellis and P. Ros, *Chem. Phys.*, 1973, **2**, 41-51.
9. J. L. Whitten, *J. Chem. Phys,*, 1973, **58**, 4496-4501.
10. M. Feyereisen, G. Fitzgerald and A. Komornicki, *Chem. Phys. Lett.*, 1993, **208**, 359-363.
11. O. Vahtras, J. Almlöf and M. W. Feyereisen, *Chem. Phys. Lett.*, 1993, **213**, 514-518.
12. A. V. Marenich, C. J. Cramer and D. G. Truhlar, *J. Phys. Chem. B*, 2009, **113**, 6378-6396.
13. S. Grimme, *Wiley Interdscip. Rev. Comput. Mol. Sci.*, 2011, **1**, 211-228.
14. S. Tobisch and T. Ziegler, *J. Am. Chem. Soc.*, 2004, **126**, 9059-9071.
15. F. Zaccaria, C. Ehm, P. H. M. Budzelaar and V. Busico, *ACS Catalysis*, 2017, **7**, 1512-1519.
16. F. Zaccaria, R. Cipullo, P. H. M. Budzelaar, V. Busico and C. Ehm, *J. Polym. Sci., Part A: Polym. Chem.*, 2017, **55**, 2807-2814.